2018

In vivo characterization of hippocampal electrophysiological processes in the heterozygous Pten knockout model of autism

Anthony J. Spinella
University of Vermont

Matthew Weston
University of Vermont

Jeremy Barry
University of Vermont

In Vivo Characterization of Hippocampal Electrophysiological Processes in the Heterozygous Pten Knockout Model of Autism

Anthony Spinella

University of Vermont

Thesis Committee Members

Jeremy Barry

Sayamwong Hammack

Donna Toufexis

Matthew Weston

IN VIVO CHARACTERIZATION OF PTEN KO (+/-) CA1 NEURONS

Abstract

While cognitive deficits have been described in the heterozygous Pten (+/-) KO mouse model of autism, little work has been done to demonstrate how corresponding *in vitro* physiological alterations in this model may underpin these cognitive deficits *in vivo*. We attempt to bridge this gap between cognitive and physiological dysfunction by measuring the efficacy of hippocampal networks through the *in vivo* recording of CA1 place cells. As Pten KO (+/-) is known to alter electrophysiological characteristics of neurons *in vitro*, this study measures the *in vivo* electrophysiological characteristics of CA1 interneurons, pyramidal cells, and place cells which may underlie the spatial cognitive deficits seen in the model. Four transgenic conditional heterozygous $Pten^{+/loxPloxP}$;*Gfap-cre* mice (HetPten) and four homozygous Pten littermate control mice were used in this study. This transgene drives cre expression and excision of the *Pten* gene in hippocampal granule cells of the dentate gyrus, and neurons in CA2 and CA1, but not astrocytes. *In vivo* local field potentials and single cell recordings were made in CA1 of each mouse during an open field foraging task in two distinct arenas. HetPten mice were found to have increased interneuron and pyramidal cell firing rates. In addition, place cells demonstrated abnormal properties including increased out-of-field firing rates, an increased number of fields, and trends towards larger field sizes that were less stable in comparison to controls. HetPten mice had slower CA1 fast gamma oscillations and more variable speed/theta oscillation correlations. Behaviorally, there were weak trends towards decreased motor output compared to controls. These data suggest that the electrophysiological alterations due to Pten KO (+/-) in mouse hippocampal neurons lead to hyperactivation of CA1 interneurons, pyramidal cells, and place cells. Rectifying these abnormal network conditions through a Pten rescue may represent a possible avenue for therapeutic intervention in the Pten KO (+/-) model.

Introduction

Autism spectrum disorders (ASD) are a set of neurological disorders characterized by repetitive movements, deficits in social interactions, and other cognitive impairments that can range from mild to severe and affect up to 1.5% of children in the United States (American Psychiatric Association, 2013; Christensen et al., 2016). Sibling studies have shown that families that have had their first child diagnosed with an ASD have up to a 26% chance of having a second child with an ASD, ASD-related language delay, deficits in social skills, or deficits in communication skills, thus highlighting the underlying genetic component to ASD (Constantino, Zhang, Frazier, Abbacchi, & Law, 2009). Nearly 46% of ASD families have been found to have gene copy number variations not seen in non-ASD families and a recent meta-analysis identified 103 known genes associated with ASD (Marshall et al., 2008; Betancur, 2012). One of these underlying genes codes for the phosphatase and tensin homolog enzyme (Pten).

In humans, Pten mutations have been implicated in up to 8.3% of ASD and a majority of which are heterozygous mutations affecting only a single allele of the *Pten* gene (Varga, Pastore, Prior, Herman, & McBride, 2008; McBride et al., 2010). Frazier et al (2015) found that in a cohort of 31 germline heterozygous Pten-ASD patients, 41% of Pten mutations were *de novo*, 24% were inherited, and 35% had no known inheritance. Additionally, the group found that 51.6% of the mutations were missense, and all the mutations led to a decrease in Pten expression. Clinically, heterozygous Pten-ASD patients have increased brain volume and white matter volume, subsequently leading to macrocephaly (Varga et al., 2009; Frazier et al., 2015). Additionally, heterozygous Pten-ASD is associated with cognitive deficits as indicated by decreased full-scale, verbal, and non-verbal IQ scores (Frazier et al., 2015).

In vitro and Pten KO mouse models have been useful in studying the effects of Pten mutations, although more work has gone into investigating the effects of homozygous Pten KO as opposed to heterozygous Pten KO models (Kwon et al., 2001; Clipperton-Allen & Page, 2014; Weston, Chen, & Swann, 2012). Heterozygous Pten knockout mice, however, have macrencephaly and deficits in social and spatial behavior, correlating to the symptomology and heterozygosity in the human condition (Page, Kuti, Prestia, & Sur, 2009; Kwon et al., 2006).

Pten is a critical enzyme in the mechanistic target of rapamycin (mTOR) signaling pathway. This pathway functions in the regulation of protein synthesis through the activation of S6K1, an enzyme involved in protein translation, and the inhibition of 4E-BP1, an enzyme that inhibits the formation of the 5' guanine cap on pre-mRNA transcripts (Brown et al., 1994; Holz, Ballif, Gygi, & Blenis, 2005; Hara et al., 1997). In the mTOR pathway, insulin receptor signaling activates P13K to convert PIP2 into PIP3 which then binds with PDK1 to activate the enzyme Akt (Volinia et al., 1995). Akt inhibits TSC1 and TSC2 which disinhibits their target (Rheb) to activate mTORC1 (Inoki, Li, Zhu, Wu, & Guan, 2002) (Figure A1).

Pten acts as an early negative regulator of the mTOR pathway as it converts PIP3 to PIP2, thus reducing the concentration of intracellular PIP3 and limiting its downstream activation of mTORC1 (Cantley & Neel, 1999; Stambolic et al., 1998) (Figure A1). This action prevents the mTOR pathway from becoming hyperactive while a loss of Pten function, such as through an inactivating mutation or heterozygous knockout, leads to mTOR hyperactivity and dysregulated protein synthesis (Lu et al., 1999; Weston, Chen, & Swann, 2012). This dysregulation in both heterozygous and homozygous Pten KO leads to an increase in neuronal cell body size (Kwon et al., 2001; Weston, Chen, & Swann, 2012; Chen, Huang, Sejourne, Clipperton-Allen, & Page, 2014).

Cell body size in neurons is directly proportional to its membrane capacitance, with an increase in soma size leading to an increase in membrane capacitance. The membrane capacitance of a neuron is inversely proportional to the membrane resistance, thus, according to Ohm's law (V = IR), it is inversely proportional to the membrane voltage. With an equivalent input current to the membrane, such as a postsynaptic current generated from the opening of postsynaptic ionotropic channels, the resulting excitatory postsynaptic response will be of smaller magnitude in a larger neuron compared to a smaller neuron. Consequently, a greater current input is necessary for a larger neuron to change the membrane voltage to the equivalent magnitude on a smaller neuron.

Conversely, *in vitro* neurons with homozygous Pten KO have been shown to make an increased number of synapses which may underlie the increased white matter volume seen in the human condition (Weston, Chen, & Swann, 2012; Frazier et al., 2015). Additionally, homozygous Pten knockout neurons have been shown to increase the evoked response in postsynaptic excitatory and inhibitory neurons (Weston, Chen, & Swann, 2012; Vogt, Cho, Lee, Sohal, & Rubenstein, 2015). In cortical parvalbumin interneurons, homozygous Pten KO leads to an increase in post-synaptic currents on layer one cortical pyramidal cells by nearly a factor of two (Vogt et al., 2015). Tonic stimulation of presynaptic glutamatergic neurons with a homozygous Pten KO has been shown to increase the spiking rate of postsynaptic neurons relative to controls. This is due to an increase in the number of releasable synaptic vesicles released into the synaptic cleft, an increase in the miniature event size, and an increase in the number of synapses formed by affected neurons (Weston, Chen, & Swann, 2012; Weston, Chen, & Swann, 2014).

Pten also influences dendritic morphology, as inhibited Pten activity leads to increased dendritic arborization, increased density of mature mushroom spines in the dentate gyrus, and a decreased number of immature thin dendritic spines (Jaworski, Spangler, Seeburg, Hoogenraad,

& Sheng, 2005; Haws et al., 2014). These physiological alterations manifest as an overall increase in synaptic transmission in homozygous Pten KO neurons, leading to an increased excitation in excitatory neurons and increased depression of postsynaptic targets in inhibitory neurons, characteristics that can influence the activity of a neuronal network (Weston, Chen, & Swann, 2014; Vogt et al., 2015).

Neural networks represent a precise balance of regulated connectivity between neurons in respect to the number of synapses made in the network, the magnitude of those connections, the timing of inputs and outputs, and the balance between network level excitation and inhibition. Altering the electrophysiological characteristics of the neurons in a network and their synaptic transmission dynamics, as what occurs with a knockout of Pten, has critical implications for the functionality of a neural network.

One of the most characterized neural networks is the hippocampal circuit which consists of inputs originating from layer two of the entorhinal cortex that synapse in the dentate gyrus and CA3 (Ramón y Cajal 1893; Steward & Scoville, 1976). Dentate gyrus granule cells then send mossy fibers that synapse on CA3 pyramidal cells which have autosynaptic connections and send Schaffer collaterals that synapse in the stratum radiatum on the apical dendrites of CA1 pyramidal neurons (Ramón y Cajal 1893; Blackstad, Brink, Hem, & June, 1970; Ishizuka, Weber, & Amaral, 1990). CA1 then sends information to both layer five of the entorhinal cortex and the subiculum, the latter of which then sends information to layer five of the entorhinal cortex, completing the cyclical perforant pathway. Layer three in the entorhinal cortex also makes a reciprocal connection with CA1 which directly synapses in the stratum lacunosum-moleculare on the apical dendrites of CA1 pyramidal cells (Lorente 1934; Naber, Silva, & Witter, 2001). The hippocampal network has primary functions in sequence generation, pattern separation, learning, and memory processes,

including those involving spatial information and Pten, as part of the mTOR pathway, has been implicated in these cognitive processes (Fortin, Agster, & Eichenbaum, 2002; Banko, Hou, Poulin, Sonenberg, & Klann, 2006).

Spatial cognition is an emergent phenomenon from the integration of signals from the spatial encoding system which includes grid cells, head direction cells, and place cells. Place cells are found in the dentate gyrus and the CA1 and CA3 regions of the dorsal hippocampus and characteristically fire in a discrete region in space within a given environment called a place field (Brun et al., 2002). Within the hippocampal place cell ensemble, each individual place field is thought to serve as a coordinate in a cognitive map that helps guide spatial behavior (O'Keefe, 1976). *In vivo*, rat place fields are stable within a given environment indefinitely and have been directly linked to spatial task performance with alterations in firing properties, such as field stability and field size, leading to decreased spatial performance (Thompson & Best, 1990; Lenck-Santini, Muller, Save, & Poucet, 2002; Liu et al., 2003). Furthermore, place fields have been shown to remap or change their firing location when moving from one context to another with different cognitive maps composed of ensemble place fields representing different contexts (Muller & Kubie, 1987; Bostock, Muller, & Kubie, 1991). Mice, on the other hand, have been shown to have reduced long-term stability for CA1 place fields as well as reduced CA1 remapping compared to rats (Kentros, Agnihotri, Streater, Hawkins, & Kandel, 2004).

CA1 place cells receive topographically organized input from both the entorhinal cortex, thought to represent real-time somatosensory input to let the animal know where it currently is in space, and CA3, thought to represent a stored representation of the particular context (Hasselmo, Bodelón, & Wyble, 2002; Naber, Silva, & Witter, 2001; Ishizuka, Weber, & Amaral, 1990). These inputs are regulated by interneurons, such as basket cells, bistratified cells, and OLM cells, that

bias the impact of either CA3 or entorhinal input on the frequency and timing of the output from CA1 pyramidal and place cells (Freund & Buzsáki, 1996). The precise timing of place cells firing within hippocampal theta oscillation, rhythmic ensemble firing patterns around five to twelve hertz, is thought to be critical for proper spatial processing and separating phases of encoding and recall (Mizuseki et al., 2009; Hasselmo & Stern, 2014; Barry et al., 2016).

Proper computation of spatial information in CA1 is dependent on the precise timing and firing of inputs from CA3 and the entorhinal cortex, proper integration of that input, and the generation of a spike output to downstream targets (Hasselmo, Bodelón, & Wyble, 2002; Naber, Silva, & Witter, 2001; Ishizuka, Weber, & Amaral, 1990). This computation depends not just on the place cells in CA1 themselves but the proper function of the entire network including both pyramidal cells and interneurons which underlie the excitation-inhibition balance of the circuit (Royer et al., 2012). Disruptions in the temporal firing pattern of inputs into CA1 place cells may disrupt communication from CA1 place cells to downstream targets that utilize that spatial information. These disruptions could stem from upstream sources such as the entorhinal cortex, CA3, dentate gyrus, which has been modeled as a pattern separator that feeds into CA1 and CA3, or from altered firing patterns from regulatory interneurons in all four regions (Heinemann et al., 2001; Neunuebel & Knierim, 2014). Santos et al. (2017) demonstrated *in vitro* that homozygous Pten KO increased excitability in mouse dentate gyrus granule cells. A question arises as to whether in vivo this increased excitability due to homozygous or heterozygous Pten KO leads to improper pattern separation and information filtering by the dentate gyrus. As different sets or patterns of visual, auditory, and olfactory stimuli define different spatial environments, improper pattern separation may lead to a reduced capacity to discern between different environments that may be indicative of the spatial deficits seen in the Pten KO model (Kwon et al., 2006).

IN VIVO CHARACTERIZATION OF PTEN KO (+/-) CA1 NEURONS

Understanding the changes in the electrophysiological properties of hippocampal neurons, especially place cells, in heterozygous Pten KO animals in comparison to controls will bridge observations of Pten KO induced alterations to morphology at the cellular level and the observed cognitive deficits at the behavioral level. If altered place field firing properties are characteristic of Pten (+/-) KO mice and these alterations result from network level abnormalities in the excitation-inhibition balance due to increased excitability and activity of heterozygous Pten KO pyramidal cells and interneurons, then correcting for the network level abnormalities may help rectify place field properties as well as improve the function of the network. If interneurons and non-place cell pyramidal cells have altered electrophysiological properties, such as increased firing rates, these may also be indicative of network level abnormalities in the excitation-inhibition balance and may also be corrected for by rectifying these network level abnormalities. A Pten rescue, whereby the excitatory effects of heterozygous Pten KO are reduced, could then lead to a restoration in the balance of excitation and inhibition at the network level in the hippocampal ensemble. This reinstatement of proper upstream inputs, such as from CA3 and the entorhinal cortex, could rectify CA1 place field firing properties thus both improving the spatial cognitive deficits in the Pten (+/-) KO model and acting as a measure for restored network functionality.

Network level activity and functionality in the hippocampus can be assessed by local field potentials in the circuit. One measure of the functionality of the hippocampus is speed/theta integration in which CA1 theta oscillations increase in frequency as mouse or rat moves faster (Richard et al., 2013; Bender et al., 2015; Blumberg et al., 2016). Pten (+/-) KO induced changes to network dynamics would disrupt this higher order integrative function of CA1. Network functionality can also be assessed through measures of slow and fast gamma oscillations which are modulated by OLM interneurons and thought to represent the routing of information within a

circuit and the interactions between pyramidal cells and interneurons (Wang & Buzsáki, 1996; Colgin & Moser, 2010). Disruptions to gamma frequencies may underlie changes in the efficacy of information processing in the heterozygous Pten KO model which manifest as spatial cognitive deficits.

This study aimed to measure altered *in vivo* electrophysiological characteristics of interneurons, pyramidal cells in mass, place cells, and local field potentials in the CA1 region of the hippocampus that arise in a heterozygous Pten (+/-) KO model of autism in mice. It was hypothesized that:

1. *In vivo* Pten (+/-) KO induced excitability of granule cells in the dentate gyrus would lead to altered CA1 place field remapping compared to controls.
2. Altered CA1 place cell remapping would be indicative of increased firing rates that accompany altered CA1 place field properties including the number of fields per cell, field size, and field coherence compared to controls.
3. CA1 pyramidal cells and interneurons would have increased firing rates compared to controls, representing a local dysregulation in the excitation-inhibition balance that disrupts CA1 place cell properties.
4. CA1 will have altered local field potentials, including theta, slow gamma, and fast gamma oscillations and changes to speed/theta correlations indicative of Pten (+/-) KO induced network level information routing alterations from CA3 and the entorhinal cortex compared to controls.

Methods

Animals:

Four transgenic conditional heterozygous *Pten*$^{+/loxPloxP}$;*Gfap-cre* mice (HetPten) with a Cre recombinase construct under the control of a modified glial fibrillary acidic protein (Gfap) promoter were used in this study. This transgenic model has been characterized previously and was chosen, as opposed to a homozygous Pten KO model, because it parallels the heterozygosity of the Pten-ASDs in humans thus allowing for better translation to the human condition (Kwon et al., 2001; Clipperton-Allen & Page, 2014). In heterozygous mice, only a single Pten allele was floxed and removed by the Cre recombinase enzyme. Expression of the transgene occurs primarily in granule cells in the mouse nervous system, such as in the dentate gyrus, but has been found to infect neurons in CA2 and CA3 as well but to a lesser extent. Virtually no astrocytes have been reported to express cre (Kwon et al., 2001). Four homozygous *Pten*$^{+/+}$*;Gfap-cre* litter control mice were used which had both functional copies of Pten intact.

Apparatus:

Two arenas were used for an open field foraging task: Arena A and Arena B. Arena A was a solid brown cardboard cylindrical arena 46.04 cm in diameter with a white cue card taped along the inside wall. The cue card spanned the height of the arena and wrapped around one-third of the arena's inner circumference. Arena B was a gray plastic cylinder with a diameter of 48.26 cm and with a white card that ran along the inner surface, spanning the height of the wall and wrapping around one-third of the arena. The white card was positioned disparately to the white card in Arena A relative to the recording room.

Preimplantation Protocol: Behavior Screening:

Prior to electrode implantation, mice were food deprived for one week to reduce their bodyweight to 85% of their pre-food deprivation bodyweight. Mice were screened in an open field paradigm. With this paradigm, each mouse was placed in Arena A for thirty-minute trials where they could freely roam (sample) the arena. Periodically, food pellets were dropped from an overhead remote feeder to promote sampling of the entire arena. At least one trial was performed for each individual mouse and trials were continually performed until the mouse became familiar with the arena and would sufficiently sample the entire arena in a thirty-minute trial window. Sufficient sampling was defined as the mouse traversing both along the edge of the arena along the wall as well as out in the center of the arena on a regular basis as mapped by video tracking of the animal. Four HetPten and four control mice met training criteria. Once they reached training criteria, mice were taken off food restriction for one week or until they returned to their pre-food restriction weight in preparation for surgical electrode array implantation.

Electrode Array Implantation:

Custom electrode implants were constructed from components obtained from Versadrive, Neuralynx, and GMW LLC allowing for *in vivo* local field potential and single cell recordings. Each electrode was comprised of four tetrode recording bundles each containing four individual recording wires, one 50-µm reference wire, and one 50-µm ground wire. Implantation surgeries were performed when the mice were between the ages of seven weeks and twenty-four weeks.

Mice were anesthetized with inhaled isoflurane and placed in a stereotaxic frame for the duration of the surgery. One electrode array was implanted into the CA1 region of the left hippocampus (AP = -2.0 mm; ML = +1.8 mm; with respect to Bregma) in each mouse. Two heterozygous Pten mice and one control mouse had a single ground wire implanted in the right cerebellum, two heterozygous Pten mice had a reference wire implanted directly into the left

cerebellum and a ground wire soldered to a skull screw inserted through the right side of the interparietal bone, and three control mice had a single ground wire soldered to a skull screw inserted through the right side of the interparietal bone. Introduction and then the unitary use of the ground wire soldered to a skull screw was found to improve the signal quality of implanted mice during behavioral recordings. The electrode arrays were anchored to the skull with Grip Cement (Dentsply Inc.) and topical antibiotics were applied to the borders of the surgical site. After the surgery, animals were given a one-week recovery period before being put back on food restriction to a bodyweight of 85% of the presurgery weight in preparation for the open field foraging task.

Post-Implantation Protocol: Open Field Foraging Task:

For the open field foraging task, mice were placed in Arena A and connected to a cable that was positioned directly above the recording arena. This cable was connected to a Neuralynx Cheetah recording system that allowed for eight-channel local field potential recordings, two per tetrode, and sixteen single unit electrode recordings, four per tetrode. Local field potential signals were preamplified at the headstage and then fed into signal amplifiers in the Neuralynx Cheetah recording system. Local field potentials were filtered at 1-9000 Hz and reference to the ground wire. Individual single unit electrode channels were referenced to another electrode channel determined per trial to be the least active.

A camera was positioned directly above the arena that tracked an LED light attached to the connection point of the cable to the electrode implant. Mice freely sampled the arena until either sufficient sampling was achieved (~ 20 minutes) or it was determined that sufficient sampling would not be achieved in which case the trail was not analyzed. Sufficient sampling was defined as the animal traversing both along the edge of the arena along the wall as well as out in the center

of the arena on a regular basis as indicated by a heat map of the recorded trajectory. Insufficient sampling was defined as the animal remaining stationary for extended periods of time, was exclusively performing thigmotaxic behavior, or only moving around the center of the arena. Food pellets were periodically dropped from an overhead remote feeder to promote sampling of the entire arena.

After the first trial in Arena A, mice were taken out of the arena and placed in their homecage for a five to ten-minute rest period. Mice were then placed back into Arena A for a duplicate trial. After the duplicate trial, mice were placed back in their homecage for a five to ten-minute rest period while Arena A was swapped from Arena B. Mice were placed into Arena B for a third trial for a minimum of twenty minutes to mimic the Arena A trials. After the first Arena B trial, mice were placed in their homecage for a five to ten-minute rest period before being placed in Arena B again for a duplicate trial. The full behavioral sequence consisted of all four trials: A1, A2, B1, and B2.

After a recording sequence, each tetrode was manually lowered such that new cells could be recorded. Recording sessions were halted when either the tetrodes could not be lowered any further or the recording site was determined to be beyond the CA1 region of the hippocampus.

Histology:

Upon completion of the electrophysiological recordings from each respective mouse, each mouse was perfused to allow for slice analysis to verify that recordings were made in the dorsal CA1 region of the hippocampus. Perfused brains were set in OCT and sectioned in 30 μm sections on a cryostat. Cresyl violet staining was performed to identify the lesion tracks of the electrode array wires in the mouse brain. First, the sections were washed in distilled water for fifteen seconds, then incubated for five minutes in a cresyl violet stain, then incubated in successive thirty-

second intervals in 70% ethanol, 95% ethanol, and 95% ethanol-glacial acetic acid solutions. The sections were then placed in 100% ethanol for ninety seconds before two one-minute incubations in xylene. The sections were then allowed to set for seventy-two hours before imaging on a light microscope. This analysis confirmed all recordings were from the CA1 region of the left hippocampus (see Figure 2A for an example cresyl violet stain).

Motor Baseline Open Field Task:

Baseline motor behavior was measured through positional tracking in an open field maze. Four additional, unimplanted HetPten mice and four litter control mice were used. All mice were between five and six weeks old. No mouse was implanted or put on food restriction at any point during the experiment. On day one, each mouse was placed into Arena A and allowed to freely sample the arena for two thirty-minute sessions. On day two, each mouse was placed into Arena A for two additional thirty-minute sessions. No food pellets were dropped to encourage sampling on either day. Position measurements recorded by a camera positioned directly over the arena and were analyzed by custom software (Biosignal, Brooklyn).

Data Analysis:

Post Implantation Open Field Foraging Task: EEG Spectral Analysis:

One EEG channel was taken per tetrode that had at least one recorded pyramidal cell, place cell, or interneuron in A1 and B1 sessions. The EEG spectral analysis was performed with a custom MATLAB software for fast and slow theta (5 -12 Hz), slow gamma (25 – 50 Hz), and slow gamma (65 – 140 Hz) frequencies along the following parameters: mean frequency, peak frequency, normalized mean frequency amplitude, and peak frequency amplitude. Mean frequency and normalized mean frequency amplitude analyses were performed across the respective frequency band for slow gamma, fast gamma, and combined fast and slow theta frequencies. The mean

frequency amplitude was normalized to minimize the bias of EEG recording site depth within CA1 on frequency amplitudes.

Post Implantation Open Field Foraging Task: Single Unit Recordings:

Single unit recordings from the open field foraging task were initially analyzed with the cell clustering program Offline Sorter (version 2.8.8., Plexon Inc) to define which recorded action potentials corresponded to either a particular pyramidal cell or interneuron based on recorded waveform properties. All relevant spiking units were then analyzed with a custom MATLAB program. Interneurons were analyzed in terms of mean firing rate. Mean firing rate was defined as the number of action potentials per second across an entire arena across an entire trial length.

The pyramidal cells were analyzed to determine their firing coherence and mean firing rate. Coherence represented a measure of how similar the firing rate of a binned pixel representing a discrete area within an arena was with the firing rates of its neighboring pixels. The overall coherence is an average of each individual pixels' coherence.

A subset of the pyramidal cells was separately classified and analyzed as place cells if they had an observed placed field based on the following criteria: in at least one session in a recording series, the cells had a coherence of ≥ 0.24, ≥ 9 contiguous pixels with spiking activity, a mean firing rate ≤ 2.6 Hz, and a field size that did not encompass the entire arena. Place cells were analyzed in terms of the number of place fields, coherence, out-of-field, infield, and mean overall firing rates, field size, and field stability. Out-of-field firing rate was defined as the mean firing rate across all non-place field pixels, infield firing rate was defined as the mean firing rate across all place field pixels, and mean overall firing rates were defined as the mean firing rate across all pixels within the arena. Field size was defined as the number of pixels that comprised the largest place field per cell per session. Field stability was defined as a function of how similar the firing

rate for a discrete region of an arena was between two sessions. This was calculated by averaging the pixel-pixel rate correlation across all corresponding pixels between pairs of sessions (A1A2, A1B1, A1B2, A2B1, A2B2, and B1B2).

Motor Baseline Open Field Foraging Task:

Baseline motor behavior for unimplanted HetPten mice and control mice was analyzed along the following parameters: total path traveled, average running speed, and trajectory linearity. The total path traveled represented the total distance (m) the mouse made during the thirty-minute trial. Average running speed (cm/s) was defined as the total distance the mouse traveled (cm) divided by the trial time (1800 seconds). Trajectory linearity was used as a measure of annular motion during each sampling session, with a value of one representing a perfectly linear trajectory and values approaching zero representing increasingly annular motion.

Statistical Analysis:

Statistical analyses were performed with SPSS. A generalized estimating equation (GEE) with a gamma log-link distribution was used to determine statistical significance by animal between groups (HetPten vs. control) across sessions (A1, A2, B1, and B2). This was done for EEG analyses, pyramidal cell mean firing rates, place cell infield, out-of-field, and mean overall firing rates, coherence, field size, and field stability, and the baseline behavior parameters. GEEs are a type of regression marginal models that allow for the analysis of correlated and clustered data. A gamma with log link model was used because these variables are scalar and are skewed toward positive values in a non-normal distribution.

A GEE with a gamma log-link distribution was used to determine the statistical significance of interneuron mean firing rate by animal between groups while collapsing across sessions (HetPten vs. control mice). Sessions were used as a covariate for this analysis.

A GEE with a Poisson log-link model was used to determine statistical significance by animal between groups (HetPten vs. control) across sessions (A1, A2, B1, and B2) for the number of place fields per place cell. A Poisson log-link model was used because the number of place fields is a count variable that is skewed toward positive values in a non-normal distribution.

Results

HetPten mice have altered CA1 place field stability and remapping

In this Pten (+/-) KO model, granule cells in the dentate gyrus are a primary target of the heterozygous Pten KO leading to increased excitability in granule cells (Hasselmo, Bodelón, & Wyble, 2002; Naber, Silva, & Witter, 2001; Ishizuka, Weber, & Amaral, 1990). The dentate gyrus is involved in pattern separation including discerning between the set of sensory cues, from the entorhinal cortex, that that define one environment over another (Heinemann et al., 2001; Neunuebel & Knierim, 2014). This pattern separation would influence remapping in which one ensemble of place cells in CA1 representing an environment changes to a new ensemble when moving to a second environment. We investigated whether *in vivo* Pten KO induced excitability of granule cells in the dentate gyrus would lead to altered place field remapping in HetPten mice compared to controls.

To determine this, single unit recordings of CA1 place cells were performed on HetPten (n = 4) and control (n = 3) mice during an open field task across four sessions in two different contexts (A1, A2, B1, and B2) (for cell counts across animals see Table A1). Muller rate map and smoothed map representations of HetPten CA1 neurons reveal place field properties as seen by two example place cells recorded in P1 (Figure 1). Place Cell 1 had a defined field of firing in the center of Arena A in session A1, with little firing along the periphery of the arena and increasing firing rates toward the center of the field. This feature, coupled with the high field coherence of 0.439 (S.U.),

a mean firing rate of 0.792 Hz, and the presence of > 9 contiguous pixels in the firing range characterize this as a place field. This field is not stable, however, in A2 as the field coherence drops to 0.151 (S.U.), thus failing to meet place field criteria. In Arena B, Place Cell 1 forms a field along the upper edge of the arena with proper coherence, size, and firing rate. This place field remains stable between B1 and B2 (Figure 1A). While the relative location of the place field in Arena B was similar to Arena A, the place fields in each arena have distinct firing patterns from one another. This demonstrates remapping in Place Cell 1 as a new field was generated for the

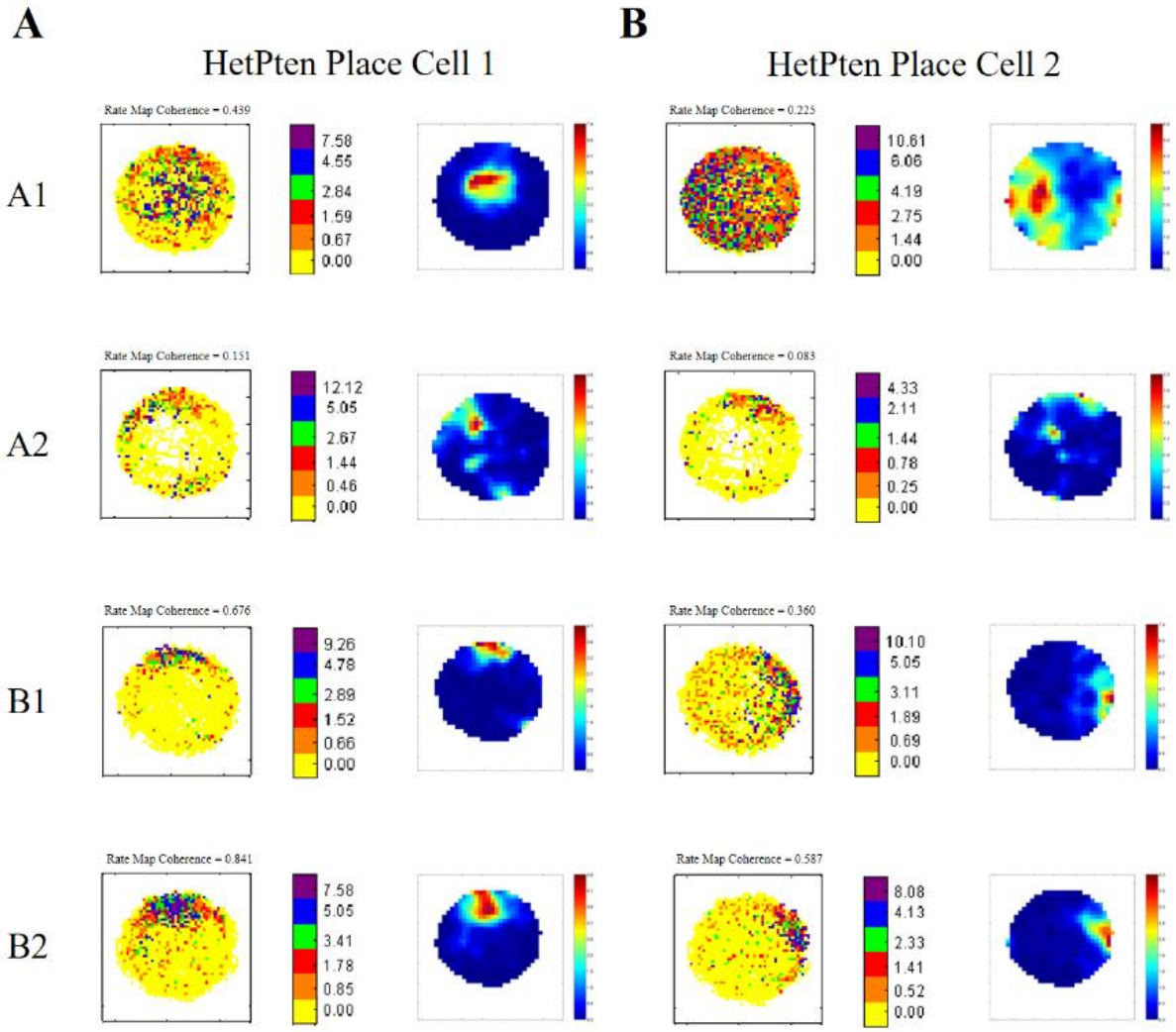

Figure 1: Muller rate maps and smoothed maps of P1 place cells (n = 2) across all four open field sessions. Muller rate maps measure the firing rate per pixel of a place cell with cooler colors representing an increased firing rate. Smoothed maps minimize lower firing rate pixels and maximize higher firing rate pixels to limit the effect of recording noise. Muller rate maps and smoothed maps were rate filtered to only firing activity when P1 was moving ≥ 5 cm/s. The place field coherence is indicated above each Muller rate map for the corresponding session (left). ***A***, Place Cell 1. ***B***, Place Cell 2.

single place cell between two different contexts, a characteristic feature of place cells. HetPten Place Cell 2, on the other hand, had no place fields in Arena A, but in Arena B, a place field emerged with a field coherence, firing rate, and size that met place field criteria in both B1 and B2 sessions. This represents another example of remapping by a HetPten place cell, as the firing field in Arena B was discrete from the firing activity in Arena A.

Muller rate map and smoothed map representations of recorded control CA1 neurons reveal place field properties as seen in two neurons (Figure 2). Control Place Cell 1 has a defined high

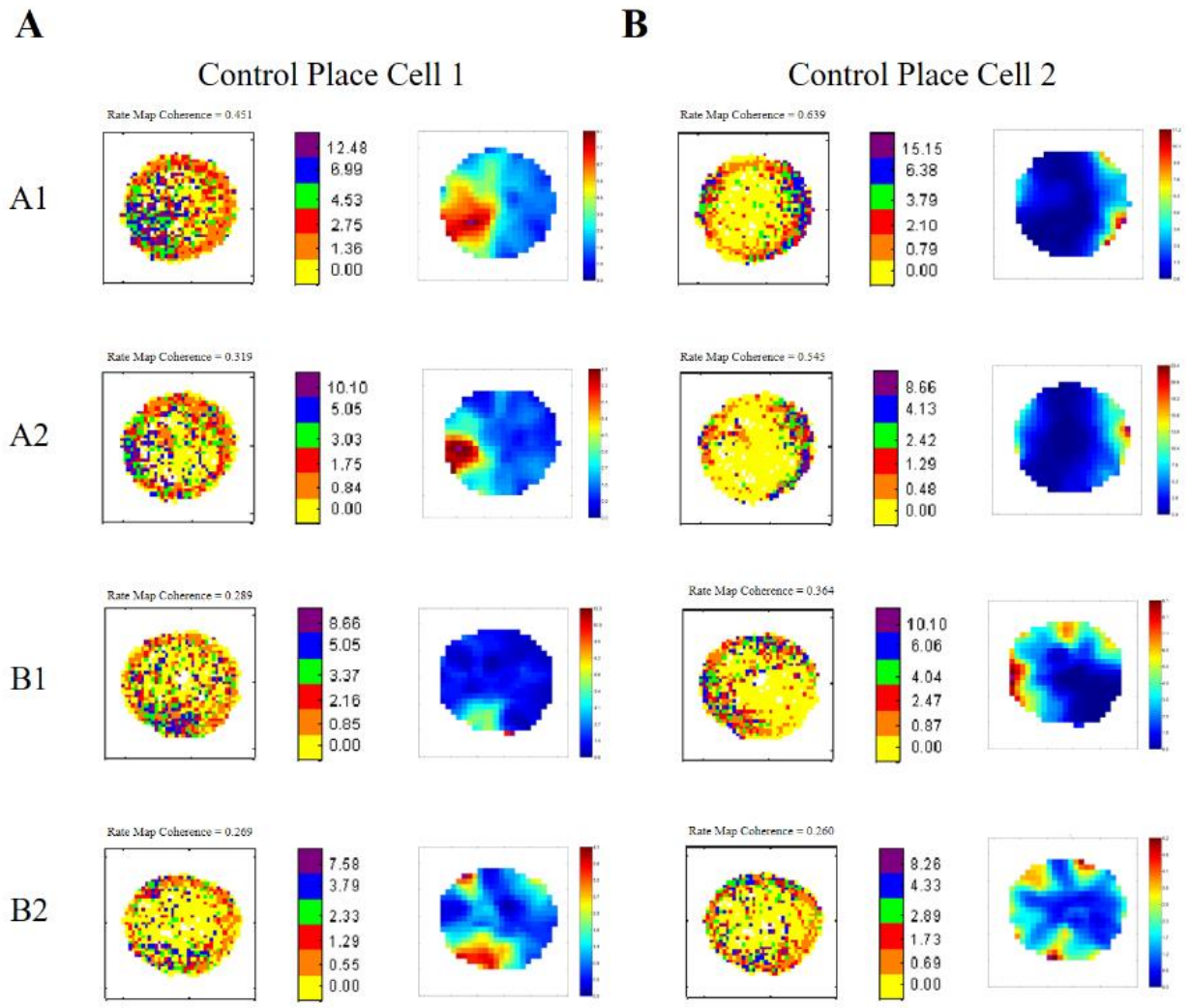

Figure 2: Muller rate maps and smoothed maps of C1 place cells (n = 2) across all four open field sessions. Muller rate maps measure the firing rate per pixel of a place cell with cooler colors representing an increased firing rate. Smoothed maps minimize lower firing rate pixels and maximize higher firing rate pixels to limit the effect of recording noise. Muller rate maps and smoothed maps were rate filtered to only firing activity when P1 was moving ≥ 5 cm/s. The place field coherence is indicated above each Muller rate map for the corresponding session (left). ***A***, Place Cell 1. ***B***, Place Cell 2.

firing rate range on the lower left quadrant of Arena A in which the highest firing rates were in the center of the field and lower firing rates along the right side of the arena. With a field coherence of 0.451 S.U., a mean firing rate of 2.376 Hz, and > 9 contiguous pixels in A1, Control Place Cell 1 met the criteria for having a place field. This field remained stable in A2 but with the context switch between A2 and B1, the field remapped to a new location along the lower edge of the arena. This field remained relatively stable in session B2 (Figure 2A). Control Place Cell 2 had a field along the right edge of Arena A and a subfield along the opposing wall which remained stable in A2. These fields then rotated during the context switch to Arena B in B1, but in B2 the field degraded into four dispersed fields along the upper right and lower left portions of Arena B. This showed that while there was adequate field stability in Arena A, the field stability in Arena B was decreased ($r = 0.1624$ between A1A2; $r = 0.0682$ between B1B2) (Figure 2B).

Place Field Stability:

When analyzing across groups, controls place cells had a greater field stability within Arena A and between sessions A2 and B1 respectively compared to HetPten place cells ($r = 0.060 \pm 0.0124$ in A1A2, and $r = 0.024 \pm 0.0060$ in A2B1 in HetPten vs $r = 0.123 \pm 0.0001$ in A1A2, and $r = 0.057 \pm 0.0015$ in A2B1 in controls, $P \leq 0.001$). HetPten place cells had an increased field stability in A1B1, A2B1, and A2B2 session pairs compared to controls though only the session pairs A1B2 and A2B2 were statistically significant ($r = 0.082 \pm 0.0179$ in A1B2 and $r = 0.059 \pm 0.0010$ in A2B2 in HetPten vs $r = 0.028 \pm 0.0003$ in A2B1 and $r = 0.037 \pm 0.0001$ in A2B2 in controls, $P < 0.001$) (Figure 3). HetPten place cells also had a higher field stability in Arena B

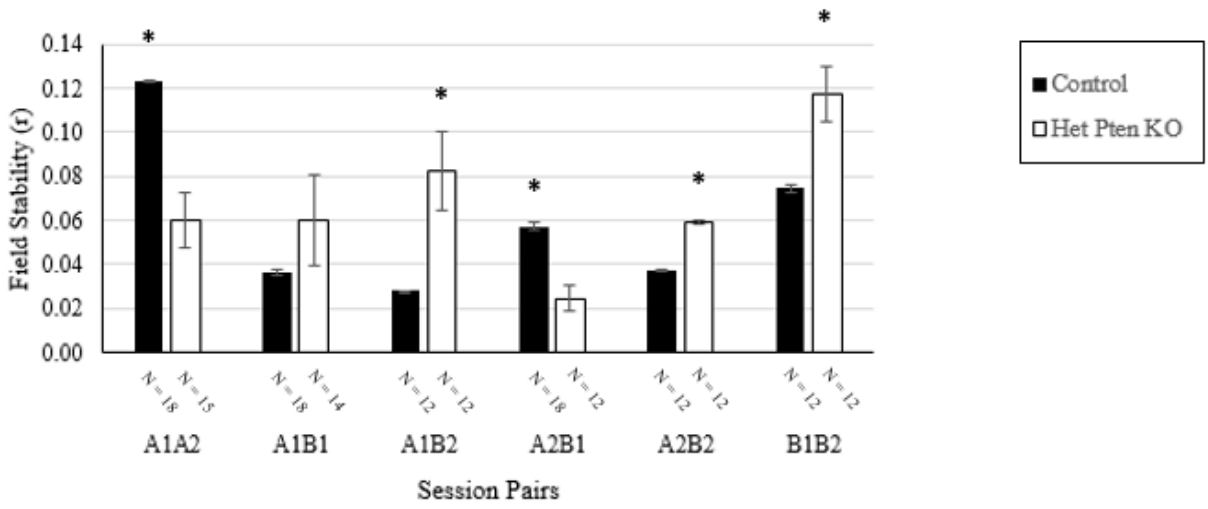

Figure 3: The mean field stability as a function of the correlation of the firing rate per pixel between the indicated session pairs. N represents the number of cells analyzed per indicated session. All error bars represent the standard error of the mean. Asterisks represent statistical significance ($P < 0.05$).

compared to controls ($r = 0.059 \pm 0.0125$ in HetPten vs $r = 0.074 \pm 0.0021$ in controls, $P < 0.001$) (Figure 3; Table A3).

HetPten mice have increased firing rates and altered place field properties

We demonstrated that HetPten mice have altered CA1 remapping properties suggesting that HetPten CA1 place fields have altered firing patterns. Pten KO has been shown to increase excitability in affected neurons *in vitro*, thus we investigated whether *in vivo* HetPten CA1 place cells had increased firing rates and whether these were accompanied by altered place field properties including the number of fields per cell, field size, and field coherence compared to controls. To determine this, single unit recordings of CA1 place cells were performed on HetPten ($n = 4$) and control ($n = 3$) mice during an open field task across four sessions in two different contexts (A1, A2, B1, and B2) (for cell counts across animals see Table A1).

<u>Infield Firing Rate:</u>

There were no statistically significant differences between the two groups for infield firing rate ($P > 0.05$) (Figure 4A).

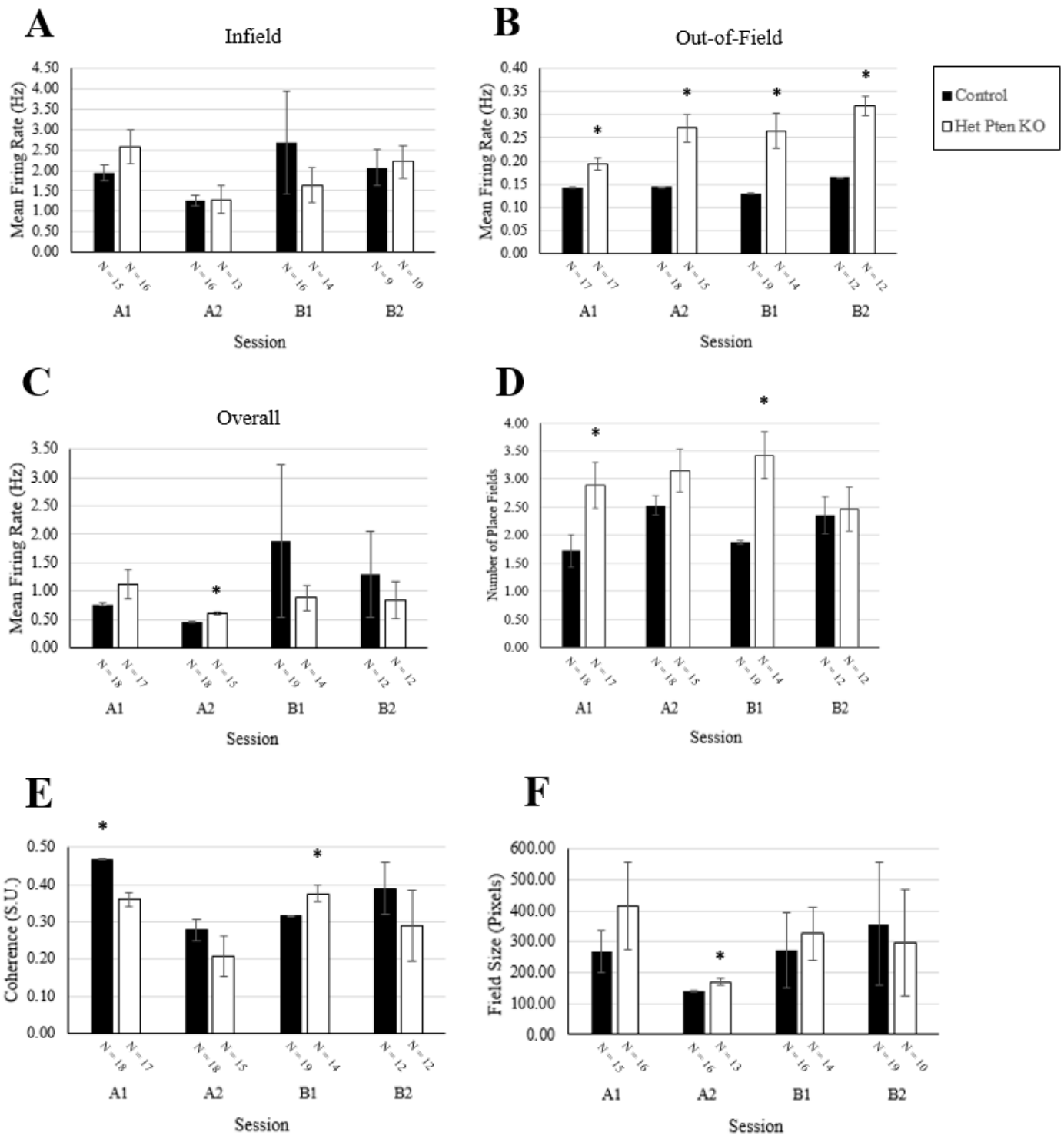

Figure 4. HetPten mice (N =4) have altered place field properties compared to controls (N = 3) across four open field task sessions in two arenas (A1, A2, B1, B2). ***A***, The mean in-field firing rate of place cells. ***B***, The mean out-of-field firing rate of place cells. ***C***, The mean overall firing rate of place cells. ***D***, The mean number of place fields per place cell. ***E***, The mean coherence of each place cell (in standard units – S.U.). ***F***, The mean size of each place field. N represents the number of cells analyzed per indicated session. All error bars represent the standard error of the mean. Asterisks represent statistical significance ($P < 0.05$).

Out-of-Field Firing Rate:

HetPten place cells had higher out-of-field mean firing rate across A1, A2, B1, and B2 compared to controls (0.195 ± 0.0132 Hz in A1, 0.272 ± 0.0.0297 Hz in A2, 0.265 ± 0.0376 Hz in B1, and 0.320 ± 0.0211 Hz in B2 in HetPten vs 0.143 ± 0.0002 Hz in A1, 0.145 ± 0.0001 Hz in A2, 0.130 ± 0.0000 Hz in B1, and 0.165 ± 0.0002 Hz in B2 in controls; $P < 0.01$) (Figure 4B).

Mean Overall Firing Rate:

HetPten place cells had a higher mean overall firing rate in A2 compared to controls (0.601 ± 0.0240 Hz in HetPten vs 0.467 ± 0.0003 Hz in controls; $P < 0.001$) and trended toward having an increased firing rate in Arena A, while in Arena B control group place cells trended toward having a higher overall firing rate though these results were not significant ($P > 0.05$) (Figure 4C; Table A2).

Number of Place Fields:

HetPten place cells had a greater number of fields across all four sessions compared to controls with a significantly greater number of fields in A1 and B1 compared to controls (2.886 ± 0.4020 in A1 and 3.422 ± 0.4208 in B1 in HetPten vs 1.723 ± 0.2900 in A1 and 1.874 ± 0.0340 in B1 in controls, $P <0.05$) (Figure 4D).

Place Field Coherence:

HetPten place cells had a decreased place field coherence across all four sessions with significant reductions in A1 and B1 compared to controls (0.361 ± 0.0193 S.U. in A1, and 0.376 ± 0.0231 S.U. in B1 in HetPten vs 0.469 ± 0.0004 S.U. in A1, and 0.315 ± 0.0003 S.U. in B1 in controls, $P <0.05$) (Figure 4E).

Place Field Size:

HetPten place cells had an increased field size in three sessions compared to controls with a statistically significant increase in A2 (171.203 ± 11.6187 pixels in HetPten vs 141.590 ± 0.1039 pixels in controls, P = 0.005). Controls had an increased field size in B2 but this result was not statistically significant (P > 0.05) (Figure 4F; Table A2).

HetPten CA1 pyramidal cells and interneurons have higher mean firing rates

HetPten CA1 place cells had altered place field properties compared to controls. These properties are regulated by the local excitation-inhibition balance of CA1 interneurons and pyramidal cells, thus, a disruption of this balance may contribute to changes in CA1 place cell properties in HetPten mice. As HetPten CA1 place cells were shown to have increased out-of-field and mean overall firing rates, we investigated whether CA1 pyramidal cells and interneurons had increased firing rates in HetPten mice compared to controls. To determine this, single unit recordings of pyramidal cells and interneurons were performed on HetPten (n = 4) and control (n

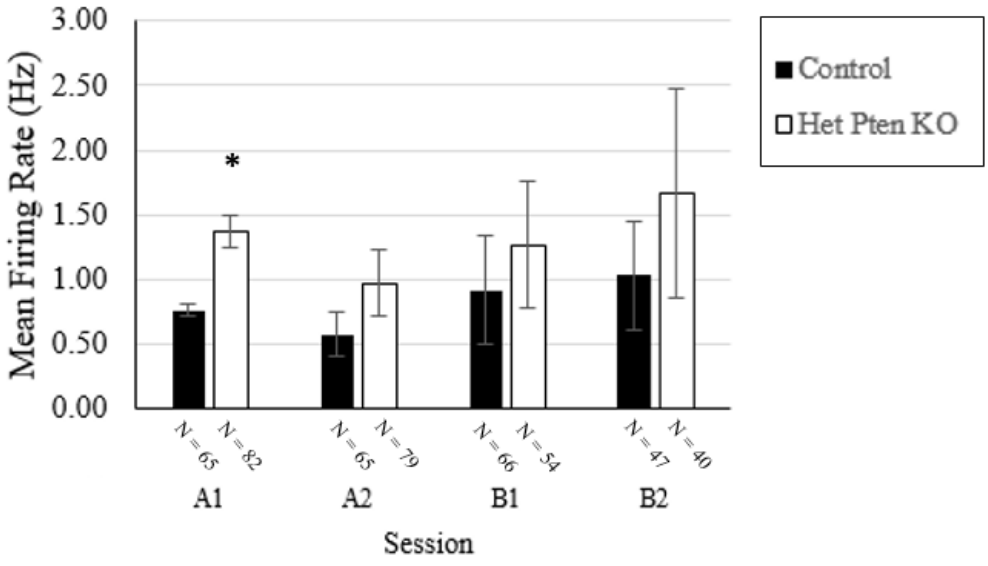

Figure 5: The mean firing rate (Hz) of CA1 pyramidal cells in four HetPten and four control mice across four sessions in two arenas (A1, A2, B1, and B2). The number of trials analyzed per session were A1 (N = 65), A2 (N = 65), B1 (N = 66), and B2 (N = 47). Error bars represent the standard error of the mean. Asterisks represent statistical significance (P < 0.001).

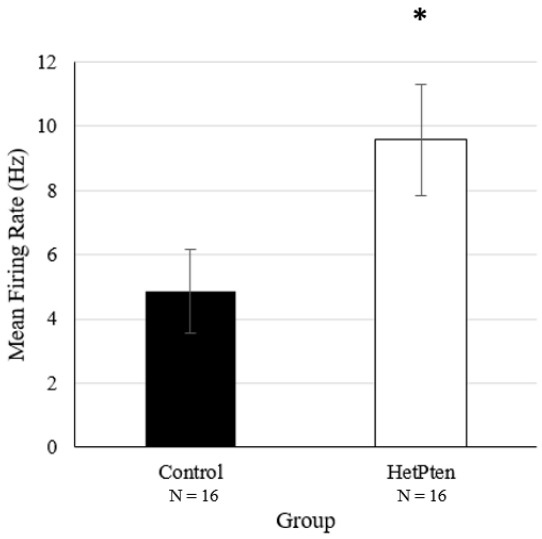

Figure 6: Mean firing rate of CA1 interneurons in HetPten and control mice collapsed across sessions. Sixteen cells were recorded and analyzed in both the HetPten (N = 4) and control groups (N = 3). HetPten CA1 interneurons fired faster than controls (P = 0.036). Error bars represent the standard error of the mean.

= 4) mice during an open field task across four sessions in two different contexts (A1, A2, B1, and B2) (for cell counts across animals see Table A1).

Pyramidal Cells:

HetPten CA1 pyramidal cells fired had a mean firing rate that was higher in A1 compared to controls (1.371 ± 0.1231 Hz in HetPten vs 0.763 ± 0.0491 Hz in controls, $P < 0.001$). HetPten pyramidal cells had trends towards higher mean firing rate across A2, B1, and B2 compared to controls though these results were not statistically significant ($P > 0.05$) (Figure 5; Table A4).

Interneurons:

When collapsing across sessions, HetPten interneurons had a mean firing rate that was higher compared to controls (9.580 ± 1.7213 Hz in HetPten vs 4.868 ± 1.2922 Hz in controls, P = 0.036) (Figure 6).

HetPten mice have slower CA1 fast gamma and more variable speed/theta correlations

On a cellular level, HetPten CA1 interneurons, pyramidal cells, and place cells are hyperactive, though these results may be indicative of disrupted network level modulation. Neural

circuits rely on a precise balance of excitation and inhibition for effective integration and computation of information (Hasselmo, Bodelón, & Wyble, 2002; Naber, Silva, & Witter, 2001; Ishizuka, Weber, & Amaral, 1990). In the hippocampus, these processes can be measured through local field potentials, such as theta and gamma oscillations which are thought to represent proper communication and routing of information between different regions of the hippocampus (Colgin & Moser, 2010). In this Pten (+/-) KO model, granule cells in the dentate gyrus and neurons in CA2 and CA3 are primarily affected, leading to hyperexcitability (Santos et al., 2017). Because these regions, in addition to the entorhinal cortex, are upstream from CA1, we investigated whether the Pten (+/-) KO induced hyperexcitability of these neurons influences the hyperactivation seen in CA1 through changes in local field potentials. To determine this, local field potentials were recorded from freely roaming HetPten (n = 4) and control (n = 4) mice during an open field foraging task in four sessions across two distinct arenas. For analysis, one EEG channel was taken per tetrode that had at least one recorded pyramidal cell, place cell, or interneuron in A1 and B1 sessions.

Theta Frequency:

No differences were found in the mean, slow peak, or fast peak of theta frequency, normalized theta frequency, or peak theta amplitude for either slow or fast theta frequencies between HetPten and control mice ($P > 0.05$) (Table A5).

Fast Gamma:

HetPten mice had a fast gamma frequency that was slower compared to controls (74.343 ± 0.5297 Hz in HetPten vs 79.531 ± 2.6040 Hz in controls, $p = 0.044$) (Figure 7). No differences were found in peak fast gamma frequency, normalized fast gamma frequency, or the peak fast gamma amplitude between HetPten and control mice ($P > 0.05$) (Table A5).

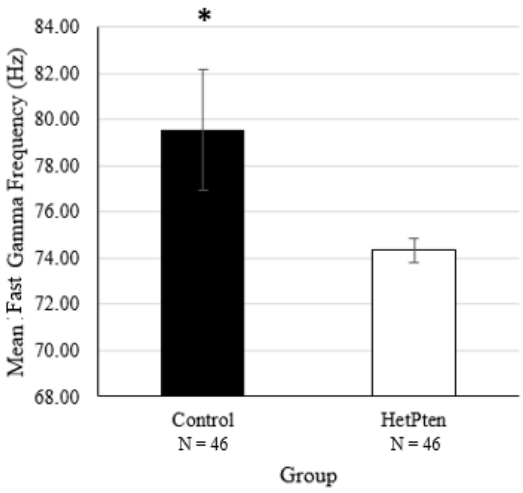

Figure 7: Mean CA1 fast gamma frequency (Hz) between HetPten and control mice collapsed across A1 and B1 sessions. Forty-six sessions were analyzed per group. HetPten mice had mean CA1 fast gamma frequency that was 7% slower compared to controls (P = 0.044). Error bars represent the standard error of the mean.

Slow Gamma:

No differences were found in either mean or peak slow gamma frequency, normalized slow gamma frequency, or the peak slow gamma amplitude between HetPten and control mice (P > 0.05) (Table A5).

Speed/Theta Correlations:

Speed/theta correlations have been shown to represent a higher order integrative process in the hippocampus in which theta oscillations increase in frequency with increasing motor speed in both rats and mice (Richard et al., 2013; Bender et al., 2015; Blumberg et al., 2016). As Pten KO has been shown to change the electrophysiological characteristics of individual neurons *in vitro*, we wanted to determine if alterations due to Pten KO (+/-) change the relationship between movement speed and CA1 theta oscillations *in vivo*. This would suggest disrupted ensemble activity in CA1 and the greater hippocampal network. Speed/theta correlations were determined by measuring theta oscillation in CA1 local field potentials in freely roaming HetPten

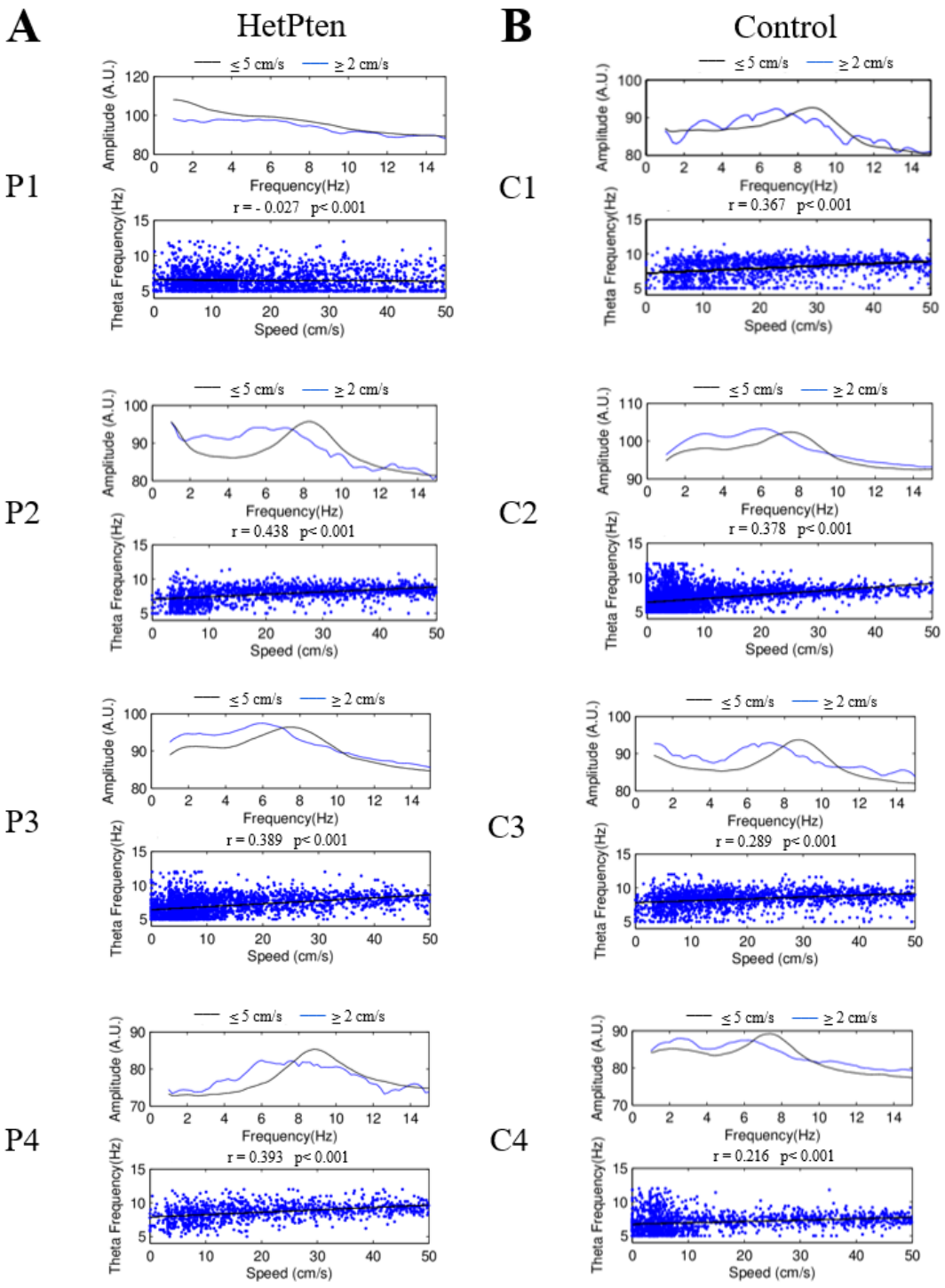

Figure 8. Example speed/theta correlation diagrams from one session for each mouse in ***A,*** the HetPten (P1, P2, P3, and P4) and ***B,*** control (C1, C2, C3, and C4) groups. For each animal, the upper graph shows the amplitude (y axis) of each oscillation frequency (x axis) when the mouse is moving less than or equal 2 cm/s (blue line) and when the mouse is running greater than or equal to five cm/s (black line). The peak amplitude within the theta oscillation range (6- 12 Hz) represents both peak slow theta (during ≤ 2 cm/s movement speed) and peak fast theta (during ≥ 5 cm/s movement speed). The lower graph plots the instantaneous theta oscillation frequency (Hz) per cycle of theta and the corresponding speed of the mouse. A Pearson's r correlation coefficient and P value are given for the trendline in the lower graph. Only HetPten mice (P1 and P4) had sessions with negative speed/theta correlations, though only 1 of 7 of these sessions was statistically significant (P <0.05).

(n = 4) and control (n = 4) mice during an open field foraging task in Arena A and Arena B. Mice were motion tracked with an overhead camera, allowing for an analysis of a mouse's instantaneous movement speed (cm/s) with respect to current theta oscillation frequency (Hz).

These data showed that there was a statistically significant speed/theta correlation for each individual mouse in both the HetPten group (P1, r = 0.165: P2, r = 0.424: P3, r = 0.374: P4, r = 0.224: $P < 0.001$) and control group (C1, r = 0.299: C2, r = 0.453: C3, r = 0.268: C4, r = 0.206: $P < 0.001$) (Figure 8). There were, however, no differences in speed/theta correlations between the HetPten and control groups (r = 0.3227 ± 0.0428 in HetPten vs r = 0.3136 ± 0.0427 in controls, $P > 0.05$) (Figure 9). While there were no differences between the mean speed/theta correlation coefficient, qualitatively the HetPten mice appeared to have more variability in speed/theta correlations both between Arena A and Arena B and within each respective arena compared to controls (Figure 10). Additionally, only two mice, P1 and P4, had negative speed/theta correlations, though only 1/7 of these individual sessions were statistically significant ($P < 0.05$). No control mice had negative speed/theta correlations.

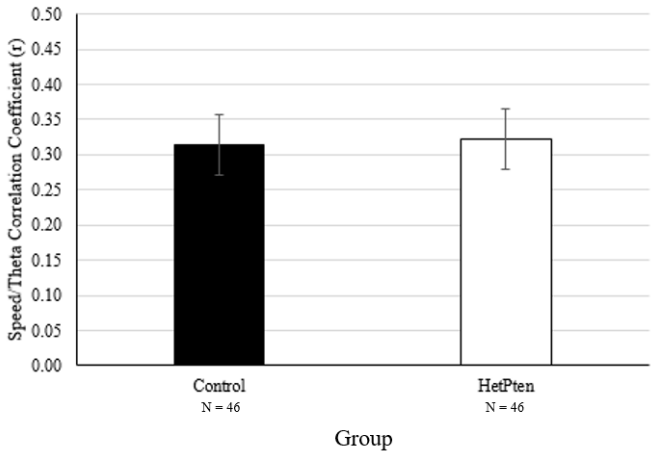

Figure 9: Mean speed/theta correlation coefficient (r) in HetPten (n = 4) and control (n = 4) mice. Movement speed was measured in cm/s and theta oscillations were measured in Hz. Forty-six sessions were analyzed for both the HetPten and control groups. There was no statistically significant difference between the groups ($P > 0.05$). Error bars represent the standard error of the mean.

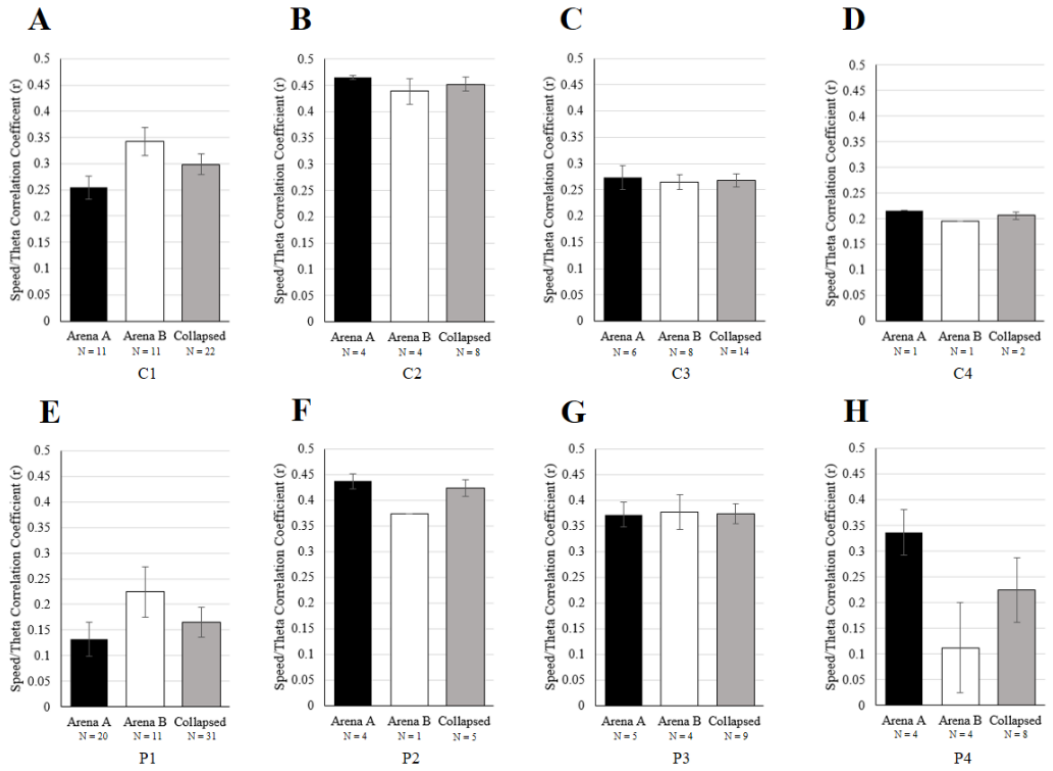

Figure 10: Speed/theta correlation coefficients for each mouse in the HetPten (***A***, P1; ***B***, P2; ***C***, P3; ***D***, P4) and control (***E***, C1; ***F***, C2; ***G***, C3; ***H***, C4) groups. N values represent the number of sessions analyzed for each mouse in Arena A, Arena B, and collapsed across both arenas. Error bars represent the standard error of the mean.

Young HetPten mice trend toward reduced motor output

During *in vivo* open field foraging task recordings, it was observed that some HetPten mice appeared to move around the arenas in a curvilinear fashion that was beyond normal thigmotaxic behavior. This behavior was seen only in the HetPten mice, in particular, a mouse (P5) that ran in the same direction so much that the connecting cable to the electrode array became compromised such that no data could be recorded.

We performed two thirty-minute trials where P5 was placed into Arena A and allowed to freely roam without being connected to the recording cable and analyzed P5's mean speed, the total path traversed, and the linearity of its trajectory. P5 had a mean speed of 14.195 cm/s, a total path traversed of 255.465 m, and a linearity of 0.245 representing a notably circular trajectory (Figure 11). Because of the high mean speed and total path traveled and the low movement

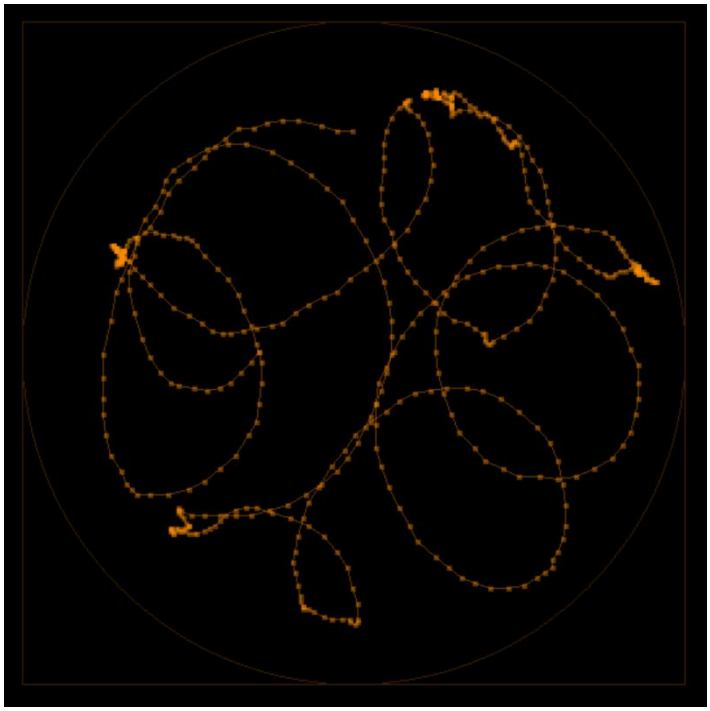

Figure 11.: The trajectory of P5 during the first twenty seconds of the second baseline behavior trial. During this trial, P5 had a mean speed of 19.29 cm/s, a total path traversed of 347.16 m, and a trajectory linearity of 0.2725.

linearity seen in P5, we investigated whether HetPten mice had an increased motor output and whether this motor output was more annular compared to controls.

To analyze the baseline behavior of HetPten mice compared to control mice, we placed unimplanted one-month old HetPten (n = 4) and control (n = 4) mice in Arena A for four thirty-minute trials. We analyzed across groups in terms of mean speed, the total path traversed, the linearity of trajectory, and the time spent in each segment of the arena. These data showed that different mice followed a different pattern of motor output across the four sessions in Arena A. When evaluating heat maps of the trajectory of each mouse across all four sessions, PB1 displayed sampling across the entire arena immediately in session one and then gradually displayed more thigmotaxic behavior, where PB1 moved only along the edge of the arena, with each subsequent session (Figure 12). PB2, PB3, CB1, and CB2 all sampled the entire arena in the first two sessions, but in the last two sessions displayed more thigmotaxic behavior (Figure 12). PB4 and CB3

displayed consistent motor output throughout all four sessions with sampling across the entire arena but with a tendency to stay closer to the edges of the arena (Figure 12). CB4 displayed thigmotaxic behavior in session one but displayed less thigmotaxic behavior through the final three sessions (Figure 12).

These qualitative evaluations of the motor output of each mouse did not provide any notable trends across groups. When analyzing linearity, mean speed, and total distance traveled across groups, these data showed a trend for HetPten to have a slower movement speed and subsequently traversing a shorter total distance across all four sessions and collapsed across

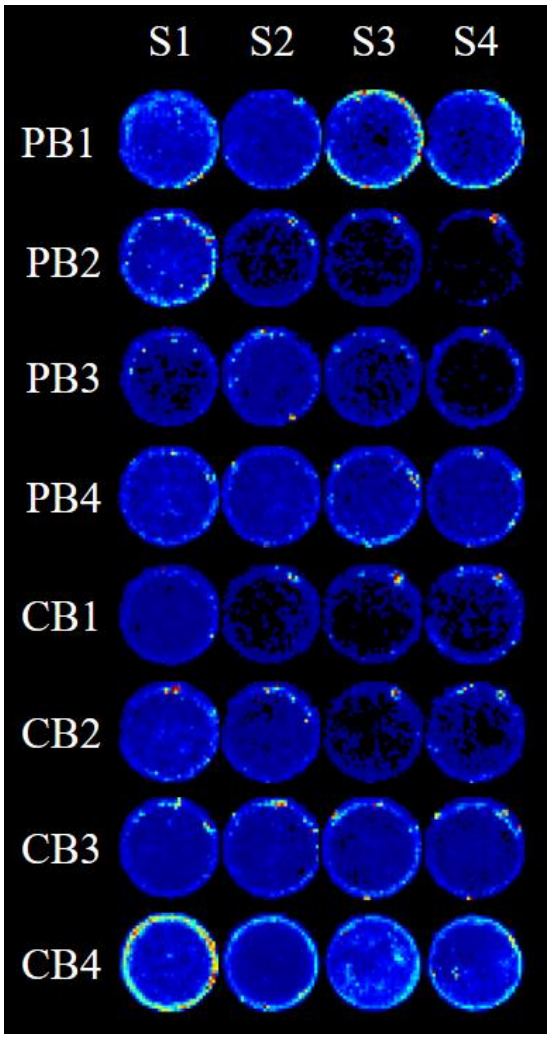

Figure 12: Position heat map in Arena A during four baseline behavior open field foraging task sessions (S1-4) for four HetPten (PB1, PB2, PB3, and PB4) and four control (CB1, CB2, CB3, and CB4) mice. Warmer colors represent an increased time spent in a location in the arena during the indicated sessions.

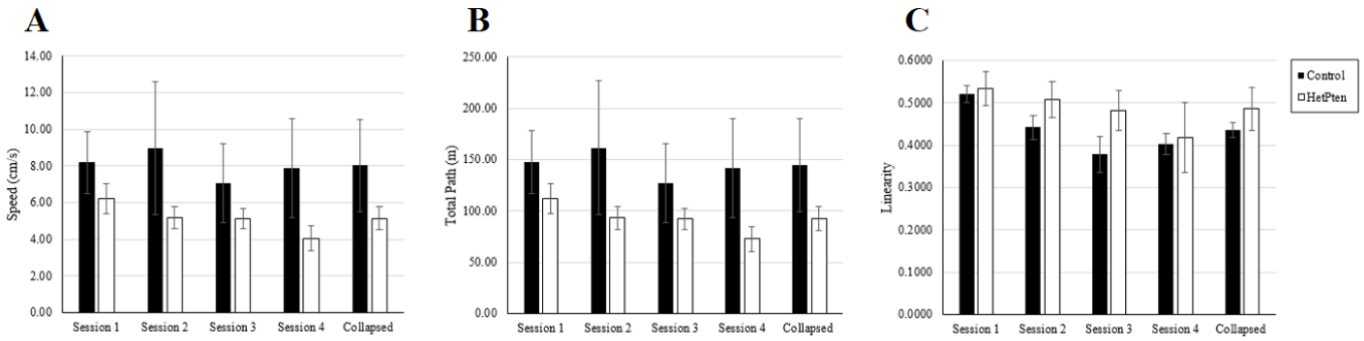

Figure 13: Baseline motor behavior characteristics in unimplanted HetPten (n = 4) and control (n = 4) mice across four sessions in Arena A. ***A***, the mean speed (cm/s) of HetPten and control mice across all four sessions and collapsed across sessions. ***B***, the total path traveled (m) of HetPten and control mice across all four sessions and collapsed across sessions. ***C***, the linearity of the trajectory of HetPten and control mice across all four sessions and collapsed across sessions. Higher linearity values represent more linear movements across the indicated sessions. There were no statistically significant differences in mean speed, total path, or linearity between the HetPten and control groups. Error bars represent the standard error of the mean.

sessions compared to controls, though these results were not statistically significant ($P > 0.05$) (Figures 13A and 13B). There were no differences in linearity between the HetPten mice and control mice ($P > 0.05$) (Figure 13C; Table A6).

Discussion

In this study, we examined the *in vivo* electrophysiological characteristics of CA1 local field potentials and CA1 interneurons, pyramidal cells, and place cells in heterozygous Pten (+/-) conditional knockout mice during an open field foraging task. HetPten mice were found to have increased CA1 interneuron and pyramidal cell firing rates while HetPten place cells had altered place field properties. These properties included increased out-of-field firing rates, an increased number of place fields per cell in both Arena A and Arena B, trends towards larger field sizes, and abnormal field stabilities compared to controls.

CA1 pyramidal cell, including place cell, hyperactivity may be indicative of poor feedback inhibition between pyramidal cells and interneurons leading to greater excitatory input onto pyramidal cells. This increased activity occurred only in out-of-field regions and not infield regions for CA1 place cells. This could be due to abnormal regulation by CA1 interneurons that do not properly silence CA1 place cells outside of their normal firing field, perhaps through poor

feedback inhibition, thus leading to an increased out-of-field firing rate and an increase in the field size itself. Increased activity could also underlie the increased number of fields calculated per CA1 place cell as their increased out-of-field firing rate may allowing for bundles of firing activity in other portions of the arena to meet place field criteria. A question that arises from this observation is whether those additional place fields are physiologically functional, in that they are coding for a coordinate on a cognitive map of a given environment, or if they are merely a byproduct of poor feedback inhibition. If they are functional, these additional place fields per CA1 place cell could interfere with the proper operation of functional place fields in spatial cognitive tasks, thus representing a cause of spatial cognitive deficits shown in the model (Page et al., 2009).

Another contributor to the spatial cognitive deficits in the model may lie in the differences in field stability between HetPten and control mice. *In vitro,* both excitatory and inhibitory neurons with Pten knockout have been shown to increase the firing rate of postsynaptic targets (Weston, Chen, & Swann, 2012). In this heterozygous *Pten*$^{+/loxPloxP}$;*Gfap-cre* model, granule cells in the dentate gyrus and neurons in CA2 and CA3 are primarily affected by the conditional knockout (Weston, Chen, & Swann, 2012; Weston, Chen, & Swann, 2014; Vogt et al., 2015). Here, we demonstrated that while CA1 interneurons had increased firing rates, CA1 pyramidal cells and place cells also had increased rates. In terms of place cells, this suggests that disruptions to the hippocampal ensemble upstream from CA1, such as in CA3 and in the dentate gyrus, lead to greater presynaptic input into CA1 place cells leading to increased activation.

We hypothesized that *in vivo,* the Pten (+/-) induced hyperexcitability in granule cells in the dentate gyrus would lead to a reduction in pattern separation that would manifest as altered CA1 place field remapping and stability (Heinemann et al., 2001; Neunuebel & Knierim, 2014). HetPten mice had increased field stability in four of the six session comparisons suggesting that

HetPten CA1 place fields remain stable over time. This could be detrimental for place cell remapping between two different environments where individual cells alter their firing location and rate between two different environments leading to an ensemble shift in the population of place cells representing the cognitive maps of each environment (Bostock, Muller, & Kubie, 1991; Muller & Kubie, 1987).

Increased stability across two trials in the same context would represent stable place fields and would be cognitively beneficial for the mouse, but increased field stability between two different environments would represent a reduction in remapping and indicate a reduction in the ability to separate patterns by the dentate gyrus. Pten (+/-) KO induced hyperactivity of granule cells in the dentate gyrus could result in a reduced ability to select the necessary information coming from the entorhinal cortex to establish a distinct representation for each environment for hippocampal spatial processing. This would reduce the distinction between two environments leading to less remapping by CA1 place cells and correspondingly greater stability or persistence of their place fields between the two environments. HetPten place cells had trends towards increased field stability in 75% of the inter-arena session pairs (A1B1, A1B2, and A2B2), suggesting that the place cells did not properly remap, thus underlying confusion between the two contexts due to poor pattern separation. *In vivo* single cell recordings of granule cells in the dentate gyrus, however, would be necessary to determine if they have increased firing patterns in the Pten KO (+/-) model and that these firing patterns directly correspond to reduced field remapping to support this hypothesis.

Additionally, while this study involved the *in vivo* electrophysiological recording of CA1 place cells, where both stored information from CA3 and current sensory information from the entorhinal cortex converge, future studies could elucidate the firing patterns of place cells in CA3

and granule cells in the dentate gyrus. CA3 is thought to store spatial information and then send that information to CA1 during the rising phase of theta (Hasselmo, Bodelón, & Wyble, 2002). CA3 also contains cells directly impacted by the conditional heterozygous *Pten*$^{+/loxPloxP}$;*Gfap-cre* knockout in this model. Altered interneuron, pyramidal cell, and place cell properties in CA3 may represent a failure to properly store spatial information about a given environment, thus disrupting the real-time integration of stored spatial information with real-time sensory information in a given environment in CA1 leading to impaired spatial cognition.

Furthermore, in this study CA1 local field potentials were measured in HetPten and control mice during an open field foraging task. HetPten mice were found to have identical theta, gamma, and fast gamma oscillations compared to controls except for slower CA1 fast gamma oscillations. Fast gamma oscillations in CA1 represent the routing of real-time sensory information from layer three of the entorhinal cortex to CA1 pyramidal cells, including place cells (Bragin et al., 1995; Naber, Silva, & Witter, 2001; Colgin & Moser, 2010). With a slower CA1 fast gamma oscillation in HetPten mice, CA1 place cells may not be receiving proper sensory information from the environment possibly due to dysregulation by higher firing local interneurons, such as OLM cells (Wang & Buzsáki, 1996). This could represent another cause of dysregulated field stability in CA1 place cells as too little real-time sensory information, such as salient distinguishers of two environments, is being conveyed to CA1 cells leading to abnormal remapping patterns. Alternatively, Pten KO has been associated with increased soma size, increased dendritic arborization, and changes in spine densities (Kwon et al., 2001; Jaworski, Spangler, Seeburg, Hoogenraad, & Sheng, 2005; Haws et al., 2014). Since fast gamma oscillations arises from entorhinal cortex inputs into CA1 pyramidal cell dendrites, Pten (+/-) induced dendritic changes may alter said input by changes to the dendrites' ability to integrate and filter fast gamma (Wang

& Buzsáki, 1996). These data suggest that while network level connectivity, in broad, was not altered in the HetPten mice compared to controls, HetPten CA1 and entorhinal connections were disrupted.

Additionally, while speed/theta oscillation correlations were not found to be different between HetPten and control mice in this study, HetPten mice were found to have more variable speed/theta oscillation correlations and P1 and P4 were found to have negative speed/theta oscillation correlations. Speed/theta oscillation correlations represent the relationship between increasing theta frequency with increasing running speed of the mice, thus representing a complex function of the hippocampus to integrate real-time sensory information derived internal speed calculations with ensemble CA1 theta oscillations (Richard et al., 2013; Blumberg et al., 2016).

The variability of speed/theta oscillation correlations in HetPten mice may represent the disrupted input of sensory information, such as through the fast gamma oscillations from layer three of the entorhinal cortex, to CA1 place cells. Alternatively, as the variability was more notable in two HetPten mice (P1 and P4), this result could be indicative of either a greater or fewer percentage of cells in the hippocampus being affected by the conditional heterozygous *Pten*$^{+/loxPloxP}$;*Gfap-cre* knockout leading to greater disruption to the ensemble network. *In vitro*, Pten KO neurons have been shown to have greater soma sizes (Kwon et al., 2001). Therefore, while Pten KO neurons have increased postsynaptic currents, with a greater soma size more current is needed to change membrane potentials (Kwon et al., 2006; Weston, Chen, & Swann, 2012). Thus, if most neurons have a Pten KO, the system has a means to compensate for the increased firing with most cells requiring more input. Hence, it has been hypothesized that having just a few Pten knockout neurons would lead to a greater disruption of the network as their inputs would primarily fall on wildtype neurons leading to increased activity at conceivably random nodes in

the network (Luikart, B., personal communication). In HetPten mice, where there are just few cells that have a broad influence on the network, speed/theta computations could drastically vary from context to context as in one context only one Pten KO cell may be active while in another context, after remapping, multiple Pten KO cells might be active leading to a differential impact on the network. This differential impact would change the computation capacity of the network in different environments leading to variable speed/theta correlations. A future *in vivo* study that correlated speed/theta correlations with heterozygous Pten KO (+/-) models with post hoc Pten (+/-) KO cell counts in the hippocampus could elucidate this hypothesis.

Behaviorally, we hypothesized that HetPten mice would have an increased motor output and that this motor output would be more annular compared to controls. No differences in mean speed, total distance, and linearity were found, however, between HetPten and control mice, though HetPten mice trended toward decreased mean speed. These results contrasted the behavior seen in P5 where stark movement nonlinearity (0.245 in P5 vs 0.436 in controls vs 0.486 in HetPtens) and high mean speed and total distance traversed were observed. A reason for this confound may lie in the age of the tested animals. P5 was six months old at the time of electrode implantation while the unimplanted HetPten and control mice were approximately one month old during the baseline behavior open field foraging task. Unpublished observations from the Luikart, Weston, and Barry groups suggest that motor output becomes more abnormal as the HetPten mice ages leading to decreased movement linearity and increased mean speed and total distance. A longitudinal study assessing the motor output of HetPten mice would help further elucidate this hypothesis.

The broad results of this study suggest that the electrophysiological alterations due to Pten KO (+/-) in mouse hippocampal neurons lead to hyperactivation of CA1 interneurons, pyramidal

cells, and place cells and poor pattern separation that manifested as poor CA1 place field remapping. These data are comparable with other autism models, including the fragile X syndrome model where the mental retardation protein (FMRP) is not synthesized resulting in abnormal synaptic plasticity and autism like symptoms (Radwan, Dvorak, & Fenton, 2015; Sparks et al., 2017). Sparks et al. (2017) found that while CA1 place fields and local field potentials, including gamma and theta were normal in FMRP-null mice compared to controls, there were differences in experienced-based synaptic plasticity and cross-frequency organization between theta and gamma oscillations. In the Pten KO model, affected cells have been shown to make a greater number of synapses, to express a greater number of dendritic spines, and to have greater output compared to controls, characteristics that influence synaptic plasticity (Weston, Chen, & Swann, 2012; Haws et al., 2014). Additionally, HetPten mice had few differences in CA1 local field potentials though, in the context of the FMRP-null fragile x syndrome model, it may be that dyscoordination of these local field potentials underlies reduced cognition.

More work is necessary to further characterize the *in vivo* cellular and network mechanics in CA1, CA3, and dentate gyrus, as rectifying these described abnormal conditions may represent a possible avenue for therapeutic intervention in the Pten KO (+/-) model. Use of Pten rescue treatments may help correct for the spatial deficit component of Pten autistic cognitive impairments as measured by a recovery of the firing patterns of CA1 interneurons, pyramidal cells, and place cells and the restoration of place field properties and remapping.

References

American Psychiatric Association. (2013). *Diagnostic and statistical manual of mental disorders* (5th ed.). Arlington, VA: American Psychiatric Publishing.

Banko, J. L., Hou, L., Poulin, F., Sonenberg, N., & Klann, E. (2006). Regulation of eukaryotic initiation factor 4E by converging signaling pathways during metabotropic glutamate receptor-dependent long-term depression. *The Journal of Neuroscience, 26*(8), 2167-2173. doi: 10.1523/JNEUROSCI.5196-05.2006

Barry, J. M., Sakkaki, S., Barriere, S. J., Patterson, K. P., Lenck-Santini, P. P., Scott, R. C., Baram, T. Z., & Holmes, G. L. (2016) Temporal coordination of hippocampal neurons reflects cognitive outcome post-febrile status epilepticus. *EBioMedicine, 7*, 175-190. doi: 10.1016/j.ebiom.2016.03.039

Bender, F., Gorbati, M., Cadavieco, M. C., Denisova, N.,Gao, X., Holman, C., … Ponomarenko, A. (2015). Theta oscillations regulate the speed of locomotion via a hippocampus to lateral septum pathway. *Nature Communications*, 6, 1-11. doi: 10.138/ncomms9521

Betancur, C. (2012). Etiological heterogeneity in autism spectrum disorders: More than 100 genetic and genomic disorders and still counting. *Brain Research, 1380*, 42-77. doi: 10.1016/j.brainres.2010.11.078

Blackstad, T. W., Brink, K., Hem, J., & June, B. (1970). Distribution of hippocampal mossy fibers in the rat. An experimental study with silver impregnation methods. *Journal of Comparative Neurology*, *138*(4), 433-449. doi: 10.1002/cne.90138040

Blumberg, B. J., Flynn, S. P., Barriere, S. J., Mouchati, P. R., Scott, R. C., Holmes, G. L., & Barry, J. M. (2016). Efficacy of nonselective optogenetic control of the medial septum over hippocampal oscillations: The influence of speed and implications for cognitive enhancement. *Physiological Reports*, *4*(e12048), 1-20. doi: 10.14814/phy2.12048

Bostock, E., Muller, R. U., & Kubie, J. L. (1991). Experience-dependent modifications of hippocampal place cell firing. *Hippocampus, 1*(2), 193-205. doi: 10.1002/hipo.450010207

Bragin, A., Jando, G., Nadasdy, Z., Hetke, J., Wise, K, & Buzsaki, G. (1995). Gamma (40-100 hz) oscillation in the hippocampus of the behaving rat. *Journal of Neuroscience, 15*(1), 47-60. Retrieved from: http://www.jneurosci.org/

Brown, E. J., Albers, M. W., Shin. T. B., Ichikawa, K., Keith, C. T., Lane, W. S., & Schreiber, S. L. (1994). A mammalian protein targeted by G1-arresting rapamycin-receptor complex. *Nature, 369*(6483), 756-758. doi: 10.1038/369756a0

Brun, V. H., Otnaess, M. K., Molden, S., Steffenach, H., Witter, M. P., Moser, M., & Moser, E. I. (2002). Place cells and place recognition maintained by direction entorhinal-hippocampal circuitry. *Science, 296*(5576), 2243-2246. doi: 10.1126/science.1071089

Cantley, L. C., & Neel. G. B. (1999). New insights into tumor suppression: PTEN suppresses tumor formation by restraining the phosphoinositide 3-kinase/AKT pathway. *Proceedings of the National Academy of Sciences of the United States of America, 96*(8), 4240-4245. doi: 10.1073/pnas.96.8.4240

Chen, Y., Huang, W. C., Sejourne, J., Clipperton-Allen, A. E., & Page, D. T. (2015). Pten mutations alter brain growth trajectory and allocation of cell types through elevated β-catenin signaling. *Journaling of Neuroscience, 35*(28), 10252-10267. doi: 10.1523/JNEUROSCI.15272-14.2015

Christensen, D. L., Baio, J., Braun, K. V. N., Bilder, D., Charles, J. C., Constantino, J.N., … Yeargin-Allsopp, M. (2016). Prevalence and characteristics of autism spectrum disorder among children aged 8 years. *Morbidity and Mortality Weekly Report, 65*(3), 1-23. doi: 10.15585/mmwr.ss6503a1

Clipperton-Allen, A. E., & Page, D. T. (2014). Pten haploinsufficient mice show broad brain overgrowth but selective impairments in autism-relevant behavioral tests. *Human Molecular Genetics, 23*(13), 3490-3505. doi: 10.1093/hmg/ddu057

Colgin, L. L., & Moser, E. I. (2010). Gamma oscillations in the hippocampus. *Physiology, 25*, 319-329. doi: 10.1152/physiol.00021.2010

Constantino, J. N., Zhang, Y., Frazier, T., Abbacchi, A. M., & Law, P. (2009). Sibling recurrence and the genetic epidemiology of autism. *The American Journal of Psychiatry, 167*(11), 1349-1356. doi: 10.1176/api.ajp.2010.09101470

Frazier, T. W., Embacher, R., Tilot, A. K., Koenig, K., Mester, J., & Eng C. (2015). Molecular and phenotypic abnormalities in individuals with germline heterozygous PTEN mutations and autism. *Molecular Psychiatry, 20*, 1132-1138. doi: 10.1038/mp.2014.125

Fortin, N. J., Agster, K. L., Eichenbaum, H. B. (2002). Critical role of the hippocampus in memory for sequences of events. *Nature Neuroscience, 5*, 458-462. doi: 10.38/nn834

Freund, T. F., & Buzsáki, G. (1996). Interneurons of the hippocampus. *Hippocampus, 6*(4), 347-470. doi: 10.1002/(SICI_1098-1063(1996)6:4<347::AID-HIPO1>3.0.CO;2-I

Hara, K., Yonezawa, K., Kozlowski, M. T., Sugimoto, T., Andrabi, K., Weng, Q., … Avruch, J. (1997). Regulation of eIF-4EBP1 phosphorylation by mTOR. *Journal of Biological Chemistry, 272*(42), 26457-26463. doi: 10.1074/jbc.272.42.26457

Hasselmo, M. E., Bodelón, C., & Wyble, B. P. (2002). A proposed function for hippocampal theta rhythm: Separate phases of encoding and retrieval enhance reversal of prior learning. *Neural Computation, 14*(4), 793-817. doi: 10.1162/089976602317318965

Hasselmo, M. E., & Stern, C. E. (2014). Theta rhythm and the encoding and retrieval of space and time. *NeuroImage, 85*(Part 2), 656-666. doi: 10.1016/j.neuroimage.2013.06.022

Haws, M. E., Jaramillo, T. C., Espinosa, F., Widman, A. J., Stuber, G. D., Sparta, D. R., … Powell, C. M. (2014). PTEN knockdown alters dendritic spine/protrusion morphology, not density. *Journal of Comparative Neurology, 522*(5), 1171-1190. doi: 10.1002/cne.23488

Heinemann, U., Beck. H., Dreier, J. P., Ficker, E., Stabel, J., & Zhang, C. L. (1991). The dentate gyrus as a regulated gate for the propagation of epileptiform activity. *Epilepsy Research Supplement, 7*, 273-280. Retrieved from: http://www.epires-journal.com/

Holz, M. K., Ballif, B. A., Gygi, S. P., & Blenis, J. (2005). mTOR and S6K1 mediate assembly of the translation preinitiation complex through dynamic protein interchange and ordered phosphorylation events. *Cell, 123*(4), 569-580. doi: 10.1016/j.cell.2005.10.024

Inoki, K., Corradetti, M. N., & Guan, K. (2005). Dysregulation of the TSC-mTOR pathway in human disease. *Nature Genetics, 37*, 19-24. doi: 10.1038/ng1494

Inoki, K., Li, Y., Zhu, T., Wu, J., & Guan, K. (2002). TSC2 is phosphorylated and inhibited by Akt and suppresses mTOR signaling. *Nature Cell Biology, 4*, 648-657. doi: 10.1038/ncb839

Ishizuka, N., Weber, J., & Amaral, D. G. (1990). Organization of intrahippocampal projections originating from CA3 pyramidal cells in the rat. *Journal of Comparative Neurology, 295*(4), 580-623. doi: 10.1002/cne.902950407

Jaworski, J., Spangler, S., Seeburg, D. P., Hoogenraad, C. C., & Sheng, M. (2005). Control of dendritic arborization by the phosphoinositide-3'-kinase-akt-mammalian target of rapamycin pathway. *The Journal of Neuroscience, 25*(49), 11300-11312. doi: 10.1523/JNEUROSCI.2270-05-2005

Kentros, C. G., Agnihotri, N. T., Streater, S., Hawkins, R. D., & Kandel, E. R. (2004). Increased attention to spatial context increases both place field stability and spatial memory. *Neuron, 42*(22), 283-295. Doi: 10.1016/S0896-6273(04)00192-8

Kwon, C., Luikart, B. W., Powell, C. M., Zhou, J., Matheny, S. A., Zhang, W., … Parada, L. F. (2006). Pten regulates neuronal arborization and social interaction in mice. *Neuron, 50*(3), 377-388. doi: 10.1016/j.neuron.2005.03.023

Kwon, C., Zhu X., Zhang, J., Knoop, L. L., Tharp, R., Smeyne, R. J., … Baker, S. J. (2001). Pten regulates neuronal soma size: a mouse model of Lhermitte-Duclos disease. *Nature Genetics,* 29, 404-411. doi: 10.1038/ng781

Lenck-Santini, P. P, Muller, R. U., Save., E., & Poucet, B. (2002). Relationships between place cell firing fields and navigational decisions by rats. *Journal of Neuroscience, 22*(20), 9035-9047. Retrieved from: http://www.jneurosci.org/

Liu, X., Muller, R. U., Huang, L., Kubie, J. L., Rotenberg, A., Rivard, B., … Holmes, G. L. (2003). Seizure-induced changes in place cell physiology: Relationship to spatial memory. *Journal of Neuroscience, 23*(37), 11505-11515. Retrieved from: http://www.jneurosci.org/

Lorente, D. N. R. (1934). Studies on the structure of the cerebral cortex. II. Continuation of the study of the ammonic system. *Journal of Psychological Neurology, 46,* 113-177. Retrieved from: http://psycnet.apa.org/record/1935-01111-001

Lu, Y., Lin, Y., LaPushin, R., Cuevas, B., Fang, X., Yu, S. X., … Mills, G. B. (1999). The PTEN/MMAC1/TEP tumor suppressor gene decreases cell growth and induces apoptosis and anoikis in breast cancer cells. *Oncogene, 18,* 7034-7045. doi: 10.1038/sj.onc/1203183

Marshall, C. R., Noor, A., Vincent, J. B., Lionel, A. C., Feuk, L., Skaug, J., … Scherer, S. W. (2008). Structural variation of chromosomes in autism spectrum disorder. *The American Journal of Human Genetics, 82*(2), 477-488. doi: 10.1016/j.ajhg.2007.12.009

McBride, K. L., Varga, E. A., Pastore, M. T., Prior, T. W., Manickam, K., Atkin, J. F., & Herman G. E. (2010). Confirmation study of pten mutations among individuals with autism or developmental delays/mental retardation and macrocephaly. *Autism Research, 3*(3), 137-141. doi: 10.1002/aur.132

Mizuseki, K., Sirota, A., Pastalkova, E., & Buzsaki, G. (2009) Theta oscillations provide temporal windows for local circuit computation in the entorhinal-hippocampal loop. *Neuron, 64* (2), 267-280. doi: 10.1016/j.neuron.2009.08.037

Muller, R. U. & Kubie, J. L. (1987). The effects of changes in the environment on the spatial firing of hippocampal complex-spike cells. *The Journal of Neuroscience, 7*(7), 1951-1968. Retrieved from: http://www.jneurosci.org/

Naber, P. A., Silva, F. H. L., & Witter, M. P. (2001). Reciprocal connections between the entorhinal cortex and hippocampal fields CA1 and the subiculum are in register with the projections from CA1 to the subiculum. *Hippocampus, 11*(2), 99-104. doi: 10.1002/hipo.1028

Neunuebel, J. P., & Knierim, J. J. (2014). CA3 retrieves coherent representations from degraded

input: Direct evidence of CA3 pattern completion and dentate gyrus pattern separation. *Neuron, 18*(2), 416-427. doi: 10.1016/j.neuron.2013.11.017

O'Keefe, J. (1976). Place units in the hippocampus of the freely moving rat. *Experimental Neurology, 51*(1), 78-109. doi: 10.1007/BF00239813

Page, D. T, Kuti, O. J., Prestia, C., & Sur, M. (2009). Haploinsufficiency for Pten and Serotonin transporter cooperatively influence brain size and social behavior. *Proceedings of the National Academy of Sciences of the United States of America, 106*(6), 1989-1994. doi: 10.1073/pnas.0804428106

Radwan, B., Dvorak, D., & Fenton, A. A. (2016). Impaired cognitive discrimination and discoordination of coupled theta-gamma oscillations in Fmr1 knockout mice. *Neurobiology of disease, 88*, 125-138. doi: 10.1016/j.nbd.2016.01.003

Ramón y Cajal, S. (1893). Estructura del asta de Ammon y fascia dentata. *Ann Soc Esp Hist Nat, 22*.

Richard, G. R., Titiz, A., Tyler, A., Holmes, G. L., & Scott, R. C. (2013). Speed modulation of hippocampal theta frequency correlates with spatial memory performance. *Hippocampus, 23*(12), 1269-1279. doi: 10.1002/hipo.22164

Royer, S., Zemelman, B. V., Losonczy, A., Kim, J., Chance, F., Magee, J. C., & Buzsáki, G. (2012). Control of timing, rate and bursts of hippocampal place cells by dendritic and somatic inhibition. *Nature Neuroscience, 15*, 769-775. doi: 10.1038.nn.3077

Santos, V. R, Pun, R. Y. K., Arafa, S. R., LaSarge, C. L., Rowley, S., Khademi, S., … Danzer, S. C. (2017). PTEN deletion increases hippocampal granule cell excitability in male and female mice. *Neurobiology of disease, 108*, 339-351. doi: 10.1016/j.nbd.2017.08.014

Sparks, F. T., Talbot, Z. N., Dvorak, D., Curran, B. M., Alarcon, J. M., & Fenton, A. A. (2018). Normal CA1 place fields but discoordinated network discharge in a *FMR1*-null mouse model of fragile x syndrome. *Neuron, 97*(3), 684-697. doi: 10.1016/j.neuron.2017.12.043

Stambolic, V., Suzuki, A., Pompa, J. L., Brothers, G. M., Mirtsos, C., Sasaki, T., … Mak, T. W. (1998). Negative regulation of PKB/Akt-dependent cell survival by the tumor suppressor PTEN. *Cell, 95*(1), 29-39. doi: 10.1016/S0092-8674(00)81780-8

Steward, O., & Scoville, S. A. (1976). Cells of origin of entorhinal cortical afferents to the hippocampus and fascia dentata of the rat. *The Journal of Comparative Neurology, 169*(3), 347-370. doi: 10.1002/cne.901690306

Tavazoie, S. F., Alvarez, V. A., Ridenour, D. A., Kwiatkowski, D. J., & Sabatini, B. L. (2005). Regulation of neuronal morphology and function by the tumor suppressors Tsc1 and Tsc2. *Nature neuroscience, 8*, 1727-1734. doi: 10.1038/nn1566

Thompson, L. T., & Best, P. J. (1990). Long-term stability of the place-field activity of single units recorded from the dorsal hippocampus of freely behaving rats. *Brain Research, 509*(2), 299-308. doi: 10.1016/0006-8993(90)90555-P

Varga, E. A., Pastore, M., Prior, T., Herman, G. E., & McBride, K. L. (2009). The prevalence of PTEN mutations in a clinical pediatric cohort with autism spectrum disorders, developmental delay, and macrocephaly. *Genetics in Medicine, 11*, 111-117. doi: 10.1097GIM.0b013e31818fd762

Vogt, D., Cho, K. K. A., Lee, A. T., Sohal, V. S., Rubenstein, J. L. R. (2015). The parvalbumin/somatostatin ratio is increased in Pten mutant mice and by human PTEN ASD alleles. *Cell Reports, 11*(6), 944-956. doi: 10.1016/j.celrep.2015.04.019

Volinia, S., Dhand, R., Vanhaesebroeck, B., MacDougall, L. K., Stein, R., Zvelebil, M. J., … Waterfield, M. D. (1995). A human phosphatidylinositol 3-kinase complex related to the yeast Vps34p-Vps15p protein sorting system. *European Molecular Biology Organization Journal, 14*(14), 3339-3348. doi: 10.1002/j.1460-2075.1995.tb07340.x

Wang, X. & Buzsáki, G. (1996). Gamma oscillation by synaptic inhibition in a hippocampal interneuronal network model. *The Journal of Neuroscience, 16*(20), 6402-6413. Retrieved from: http://www.jneurosci.org/

Weston. M. C., Chen, H., & Swann, J. W. (2012). Multiple roles of mammalian target of rapamycin signaling in both glutamatergic and GABAergic synaptic transmission. *Journal of Neuroscience, 32*(33), 11441-11452. doi: 10.1523/JNEUROSCI.1283-12.2012

Weston, M. C., Chen, H., & Swann, J. W. (2014). Loss of mTOR repressors Tsc1 or Ten has divergent effects on excitatory and inhibitory synaptic transmission in single hippocampal neuron cultures. *Frontiers in Molecular Neuroscience, 7,* 1-15. doi: 10.3389/fnmol.2014.00001

Appendix

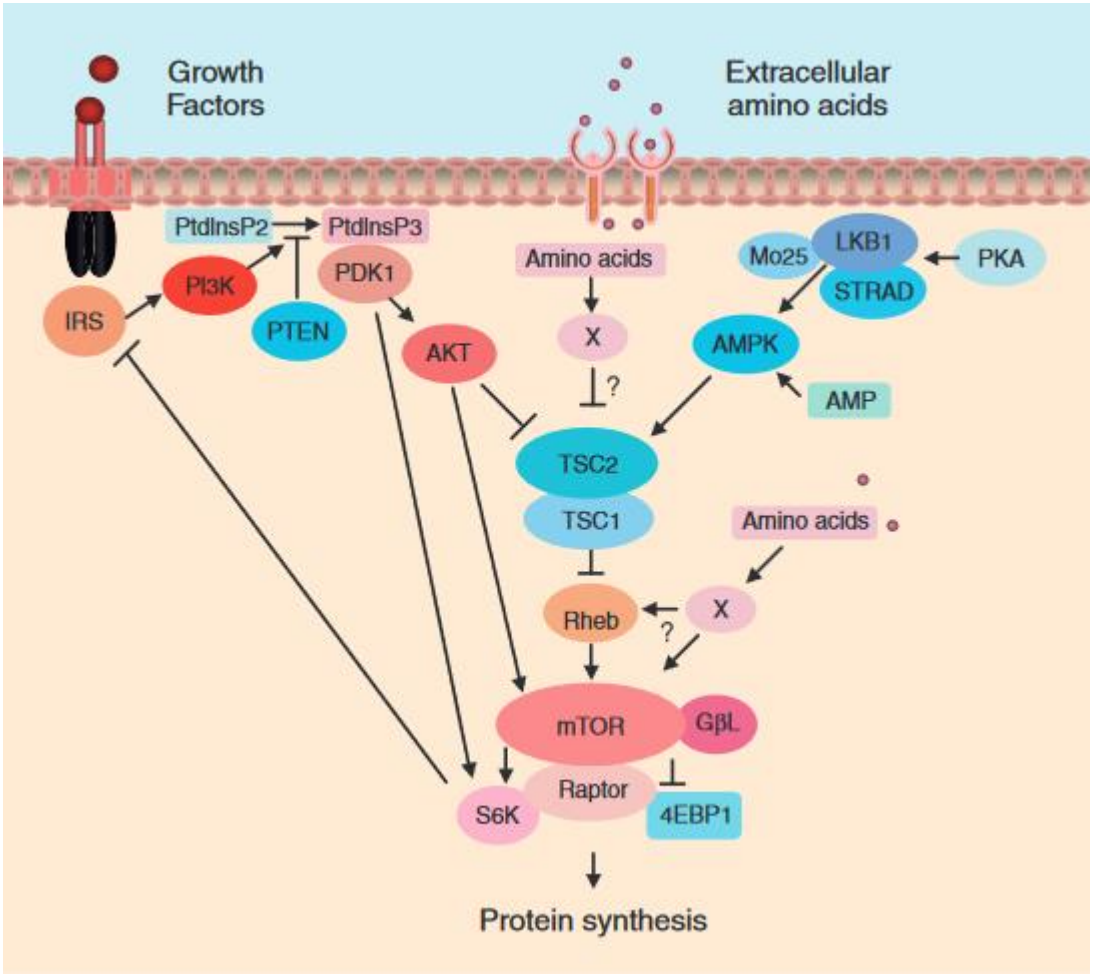

Figure A1: Schematic of the mTOR signaling pathway. Reprinted from Inoki, Corradetti, & Guan, 2005.

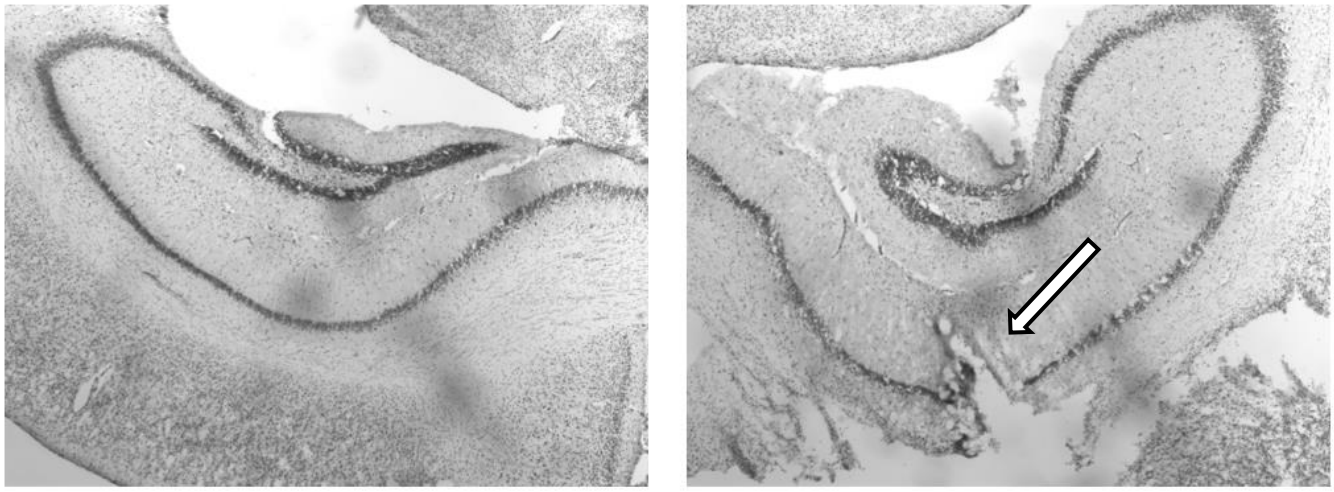

Figure A1: Cresyl violet staining of the left (on right) and right (on left dorsal hippocampus of a HetPten mouse (P2). The arrow indicates electrode tracks passing through the pyramidal cell layer of CA1 of the left hippocampus as the electrodes were lowered through successive recording sessions. Recorded units from beyond this layer were not included in analyses.

	CONTROL					HETPTEN				
	P1	P2	P3	P4	Total	C1	C2	C3	C4	Total
PYRAMIDAL CELL	53	12	11	6	82	39	4	22	1	66
PLACE CELL	8	5	2	2	17	16	1	2	0	19
INTERNEURON	10	4	1	1	16	8	3	5	0	16

Table A1: The number pyramidal cells, place cells, and interneurons recorded and analyzed from each HetPten (P1-4) and control (C1-4) mouse. Pyramidal cell counts include both place cells and non-place cell pyramidal cells.

	CONTROL		HETPTEN		
	Mean	STD Error	Mean	STD Error	P-Value
NUMBER OF PLACE FIELDS					
A1	1.723	±0.2900	2.886	±0.4020	**0.018**
A2	2.531	±0.1655	3.151	±0.3752	0.107
B1	1.874	±0.0340	3.422	±0.4208	**<0.001**
B2	2.357	±0.3255	2.462	±0.3919	0.836
PLACE FIELD COHERENCE					
A1	0.469	±0.0004	0.361	±0.0193	**<0.001**
A2	0.278	±0.0300	0.208	±0.0537	0.302
B1	0.315	±0.0003	0.376	±0.0231	**0.004**
B2	0.390	±0.0690	0.290	±0.0960	0.43
MEANING FIRING RATE					
A1	0.772	±0.0142	1.132	±0.2553	0.091
A2	0.467	±0.0003	0.601	±0.0240	**<0.001**
B1	1.888	±1.3483	0.881	±0.2280	0.316
B2	1.293	±0.7561	0.845	±0.3354	0.548
OUTFIELD FIRING RATE					
A1	0.143	±0.0002	0.195	±0.0132	**<0.001**
A2	0.145	±0.0001	0.272	±0.0297	**<0.001**
B1	0.130	±0.0000	0.265	±0.0376	**<0.001**
B2	0.165	±0.0002	0.320	±0.0211	**<0.001**
INFIELD FIRING RATE					
A1	1.939	±0.1870	2.580	±0.4247	0.135
A2	1.264	±0.1346	1.290	±0.3316	0.942
B1	2.679	±1.2640	1.640	±0.4292	0.363
B2	2.072	±0.4466	2.222	±0.4025	0.805
PLACE FIELD SIZE					
A1	268.825	±67.5166	414.510	±141.4622	0.307
A2	141.590	±0.1039	171.203	±11.6187	**0.005**
B1	272.169	±121.0958	325.861	±86.2945	0.728
B2	358.232	±197.5507	296.884	±171.3913	0.055

Table A2: CA1 place cell and place field properties for HetPten (n = 4) and control (n = 3) mice, including number of place fields, place field coherence (standard units - S.U.), meaning firing rate (Hz), out of field firing rate (Hz), in field firing rate (Hz), and place field size (pixels), across four open field foraging task sessions in two arenas (A1, A2, B1, and B2). Significant P-values ($P \leq 0.05$) are indicated in bold typeface.

	CONTROL		HETPTEN		
	Mean	**STD Error**	**Mean**	**STD Error**	**P-Value**
FIELD STABILITY					
A1A2	0.123	±0.0001	0.060	±0.0124	**<0.001**
A1B1	0.036	±0.0010	0.060	±0.0207	0.144
A1B2	0.028	±0.0003	0.082	±0.0179	**<0.001**
A2B1	0.057	±0.0015	0.024	±0.0060	**0.001**
A2B2	0.037	±0.0001	0.059	±0.0010	**<0.001**
B1B2	0.074	±0.0021	0.117	±0.0125	**<0.001**

Table A3: Place field stability for CA1 place cells in HetPten (n = 4) and control (n = 4) mice between pairs of four open field foraging task sessions in two arenas (A1, A2, B1, and B2). Statistically significant P values ($P \leq 0.05$) are indicated with bold typeface.

	CONTROL		HETPTEN		
	Mean	**STD Error**	**Mean**	**STD Error**	**P-Value**
MEAN FIRING RATE					
A1	0.763	±0.0491	1.371	±0.1231	**<0.001**
A2	0.575	±0.1741	0.974	±0.2509	0.185
B1	0.921	±0.4171	1.267	±0.4900	0.591
B2	1.037	±0.4203	1.667	±0.8103	0.453

Table A4: The mean firing rate (Hz) for pyramidal cells, including place cells, in HetPten (n = 4) and control (n = 4) mice across four open field foraging task sessions in two arenas (A1, A2, B1, and B2). Statistically significant P values ($P \leq 0.05$) are indicated with bold typeface.

	CONTROL		HETPTEN		
	Mean	**STD Error**	**Mean**	**STD Error**	**P-Value**
THETA					
MEAN FREQUENCY	7.665	±0.2480	7.772	±0.2846	0.777
PEAK - SLOW	6.452	±0.3143	6.646	±0.2767	0.644
PEAK - FAST	8.004	±0.2601	7.914	±0.3115	0.825
NORMALIZED	0.062	±0.0007	0.062	±0.0006	0.519
PEAK AMPLITUDE - SLOW	93.398	±1.6793	95.694	±1.4607	0.303
PEAK AMPLITUDE - FAST	93.382	±1.4397	95.859	±1.4312	0.223
SLOW GAMMA					
MEAN FREQUENCY	33.134	±0.6131	33.269	±0.5497	0.870
PEAK	25.953	±0.3146	25.624	±0.2275	0.397
NORMALIZED	0.188	±0.0010	0.189	±0.0009	0.500
PEAK AMPLITUDE	79.848	±1.6357	81.072	±1.4157	0.572
FAST GAMMA					
MEAN FREQUENCY	79.531	±2.6040	74.343	±0.5297	**0.044**
PEAK	65.336	±0.0504	65.316	±0.0627	0.801
NORMALIZED	0.505	±0.0031	0.502	±0.0026	0.336
PEAK AMPLITUDE	74.271	±1.3460	75.854	±1.3491	0.406

Table A5: Spectral analysis of CA1 theta, slow gamma, and fast gamma oscillations in HetPten (n = 4) and control (n = 4) mice collapsed across A1 and B1 open field foraging task sessions. Statistically significant P values ($P \leq 0.05$) are indicated with bold typeface.

	CONTROL		HETPTEN		
	Mean	**STD Error**	**Mean**	**STD Error**	**P-Value**
TOTAL PATH (M)					
S1	147.380	±30.7261	111.848	±14.5628	0.262
S2	161.488	±65.3649	93.498	±11.1110	0.195
S3	127.185	±38.7946	72.945	±9.9178	0.320
S4	141.900	±48.1704	72.945	±12.3336	0.079
COLLAPSED	144.488	±45.4658	92.616	±11.3923	0.188
MEAN SPEED (CM/S)					
S1	8.188	±1.7063	6.213	±0.8076	0.261
S2	8.973	±3.6304	5.193	±0.6174	0.195
S3	7.065	±2.1542	5.123	±0.5518	0.320
S4	7.885	±2.6769	4.050	±0.6843	0.079
COLLAPSED	8.028	±2.5254	5.144	±0.6326	0.188
LINEARITY					
S1	0.521	±0.0197	0.533	±0.0401	0.790
S2	0.442	±0.0281	0.509	±0.0426	0.183
S3	0.378	±0.0419	0.482	±0.0475	0.103
S4	0.403	±0.0256	0.419	±0.0828	0.851
COLLASPED	0.436	±0.0171	0.486	±0.0504	0.333

Table A6: Total path (m), mean speed (cm/s), and linearity measures for unimplanted HetPten (n = 4) and control (n = 4) mice across four sessions (S1-4) and collapsed across sessions in Arena A. No measure was statistically significant ($P > 0.05$).